exeley INTERNATIONAL JOURNAL ON SMART SENSING AND INTELLIGENT SYSTEMS

Article | DOI: 10.21307/ijssis-2021-003 Issue 1 | Vol. 14 (2021)

An overview of technologies and devices against COVID-19 pandemic diffusion: virus detection and monitoring solutions

R. de Fazio[1], A. Sponziello[1], D. Cafagna[1], R. Velazquez[2] and P. Visconti[1,*]

[1]Department of Innovation Engineering, University of Salento, 73100, Lecce, Italy.

[2]Facultad de Ingeniería, Universidad Panamericana, Aguascalientes 20290, Mexico.

*E-mail: paolo.visconti@unisalento.it

This paper was edited by Subhas Chandra Mukhopadhyay.

Received for publication December 21, 2020.

Abstract

The year 2020 will remain in the history for the diffusion of the COVID-19 virus, originating a pandemic on a world scale with over a million deaths. From the onset of the pandemic, the scientific community has made numerous efforts to design systems to detect the infected subjects in ever-faster times, allowing both to intervene on them, to avoid dangerous complications, and to contain the pandemic spreading. In this paper, we present an overview of different innovative technologies and devices fielded against the SARS-CoV-2 virus. The various technologies applicable to the rapid and reliable detection of the COVID-19 virus have been explored. Specifically, several magnetic, electrochemical, and plasmonic biosensors have been proposed in the scientific literature, as an alternative to nucleic acid-based real-time reverse transcription Polymerase Chain Reaction (PCR) (RT-qPCR) assays, overcoming the limitations featuring this typology of tests (the need for expensive instruments and reagents, as well as of specialized staff, and their reliability). Furthermore, we investigated the IoT solutions and devices, reported on the market and in the scientific literature, to contain the pandemic spreading, by avoiding the contagion, acquiring the parameters of suspected users, and monitoring them during the quarantine period.

Keywords

SARS-CoV-2, Pandemic, Tracking devices, RT-PCR assay, Magnetic biosensors, IoT frameworks, Spike protein, Antibodies, Remote monitoring systems.

In this research work, different innovative systems will be proposed for the detection of SARS-CoV-2. The SARS-CoV-2 virus consists of four structural proteins, namely, spike (S), envelope (E), membrane (M), and nucleocapsid (N). The name coronavirus is due to the presence of spike glycoproteins S (the S1 subunit and the S2 subunit) on its surface/envelope, just like a crown. Since the end of 2019, the COVID-19 virus has spread widely all over the world. In this field, the technology offers valid support for medical applications simplifying the work of the medical staff and improving the lifestyle of the patients (Gaetani et al., 2019, 2020; Lay-Ekuakille et al., 2019; Visconti et al., 2018). Thanks to the very recent studies carried out all over the world, we are going to have increasingly precise, portable, and non-invasive devices, which will facilitate early detection of the virus. In this way, we will be able to obtain data from a large portion of the world population, leading to a better knowledge of the deadly virus and finding a definitive cure to destroy it.

The remainder of the paper is arranged into three sections; the second section analyses the current literature related to the existing technology (e.g., magnetic biosensors, electrochemical biosensors, and plasmonic biosensors) for rapid and reliable detection

of the COVID-19 virus (Charibaldi et al., 2018). Specifically, the drawbacks of current diagnostic methods are discussed, and the advantages of biosensor-based detection over conventional ones are highlighted. These technologies could enable the development of new plug-and-play systems to manage the outbreak and prevent future ones. The third section is focused on the latest devices and techniques proposed in the literature, and already on the market, for continuously monitoring the user's vital signs, so preventing and eradicating the COVID-19 or similar diseases (de Fazio et al., 2020; Jatmiko et al., 2019; Lassoued et al., 2018; Mbuthia et al., 2018; Visconti et al., 2019; Visconti et al., 2020). The study will also focus on describing related architectures, platforms, and applications of the considered devices and technologies. The fourth section reports a comparative analysis of the technologies and sensing systems discussed in the second section , highlighting their advantages and limitations, as well as describing potentialities and emerging perspectives to make them useful solutions for facing future pandemics.

State of the art on sensors and technologies for detecting patients affected by COVID-19 virus

During the COVID-19 pandemic, the demand for high sensitivity, low-cost, rapid, easy-to-use, and reliable disease testing tools is increasing more and more. Real-Time Reverse-Transcription Polymerise Chain Reaction (RT-PCR) is the actual rapid assay used for the current diagnostic tests for the SARS-CoV-2 virus, responsible for COVID-19 disease. The RT-PCR is a complex technique that requires expensive laboratory equipment and trained technicians to perform the test and can take up to 48 h to provide results. Also, this is not a very accurate technique, as demonstrated by studies that have found up to 30% false negative.

In this paragraph, at first, we analyze the biosensor technologies and related applications. Then we look at the various diagnostic techniques of the virus through their use, trying to compare the pros and cons. Several laboratories around the world are working to find new methods and developing alternative molecular diagnostic platforms. Among the others, bio-sensing technologies, magnetoresistive biosensors, electrochemical biosensors, and plasmonic biosensors have attracted attention in the last years.

Wu et al. (2020) proposed an analysis of magnetic nano-sensors for virus and pathogen detection before COVID-19. They demonstrated that magnetic nano-sensors are more versatile and applicable for antibody, antigen, and nucleic acid detection.

In magnetic biosensors, the magnetic tags (usually magnetic nanoparticles-MNPs) are functionalized with antibodies or DNA/RNA probes that specifically bind to the target analyte. Therefore, the concentration of the target analyte is converted to the magnetic signals, generated by the magnetic tags. Compared to plasmonic, optical, and electrochemical biosensors, the magnetic ones exhibit low background noise, as most of the biological environment is non-magnetic. The sensor signal is also less influenced by the type of sample matrix, enabling accurate and reliable detection processes.

The magnetic biosensors are classified into three categories:

1. Magnetoresistance (MR) sensors,
2. Magnetic Particle Spectroscopy (MPS) platforms, and
3. Nuclear Magnetic Resonance (NMR) platforms.

MR was first discovered by William Thompson, who coined the term Anisotropic Magnetoresistance (AMR). The basic principle of MR-based devices is the variation of the resistivity of a material or a structure, as a function of an external magnetic field. Similarly, in the AMR, the resistivities of both Ni and Fe increase if the charge current is applied parallel to the magnetization direction. On the contrary, both Ni and Fe's resistivities decrease if the charge current is applied perpendicular to the magnetization direction. However, the maximum resistance variation recorded from the AMR devices is approximately only 2%, which makes it unsuitable for most applications.

The Giant Magneto-Resistance (GMR) was first observed by Albert Fert and Peter Grunberg in the Fe/Cr multi-layers grown with molecular-beam epitaxy. This multi-layer structure exhibits a resistance change more significant than that of the AMR devices. In general, the GMR effect primarily takes place in multi-layer structures with alternating ferromagnetic and non-magnetic metallic layers. When the magnetizations of two adjacent ferromagnetic layers are parallel, the multi-layer structure shows low resistance; instead, if the magnetizations are antiparallel, the structure exhibits a high-resistance. Although the GMR effect was primarily observed in a thin film or layered system, it has also been observed in other systems such as Co–Au, Co–Ag, and Fe–Ag granular films. GMR effect in granular films is strictly related to the spin-dependent interfacial scattering and inter-particle coupling, which can be exploited for biosensing purposes given their ability to adapt to the shapes of different biomolecules. Compared to other sensor types, the capability of flexible GMR sensors to respond to an external magnetic field makes them a perfect candidate for

wearable real-time body activity monitoring and the evaluation of drug-delivery effectiveness.

Baselt et al. (1998) reported the first GMR-based biosensor using the Bead Array Counter micro-array. They develop a sandwich immunoassay, shown in (Figure 1), where the capturing antibodies, specifically chosen for the target analytes (such as antigens from viruses/pathogens), are pre-functionalized on the GMR sensor surface.

Afterward, biofluid samples are added, and specific antibody–antigen bindings are created in the sensor area. Thus, the detection-antibody-functionalized MNPs are added to the GMR sensing areas, constituting the antibody–antigen–capture antibody complexes (Figure 1). Therefore, the amount of MNPs captured to the proximity of the sensor surface is directly proportional to the number of antigens in the testing sample.

Wu et al. presented a portable GMR bio-detector, called Z-Lab, able to detect the Influenza-A Virus (IAV). This bio-detector reached a Limit of Detection (LOD) of 15 ng/mL for the H1N1 virus, and a 125 TCID50/mL LOD for the purified H3N2 variant virus (H3N2v), with an overall assay time lower than 10 min (Figure 2) (Wu et al., 2017, 2020). The electronic section includes a microcontroller, a 24-bit codec, a Wheatstone Bridge for adjusting the offset on the carrier signal, a coil driver, and a USB and Bluetooth communication section.

Another research group from the Stanford University reported a similar portable GMR-based system for COVID-19 assays, shown in Figure 3, detecting the human immunoglobulin G and M (IgG and IgM) antibodies with sensitivities in the range from 0.07 to 0.33 nM (Choi et al., 2016).

The detection system includes three main components, namely the reader station, disposable

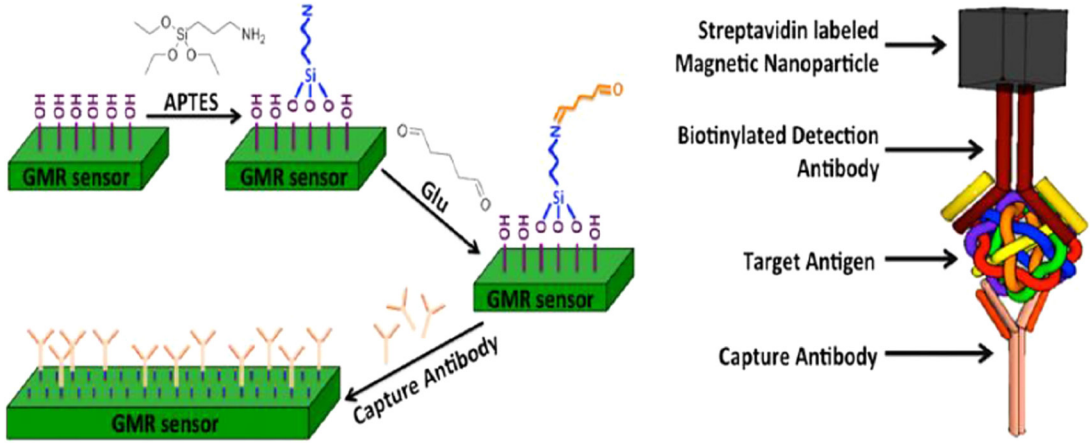

Figure 1: Sandwich immunoassay mechanism of a GMR biosensor forming a capture antibody–target antigen–detection antibody–MNP complex (Wu et al., 2020).

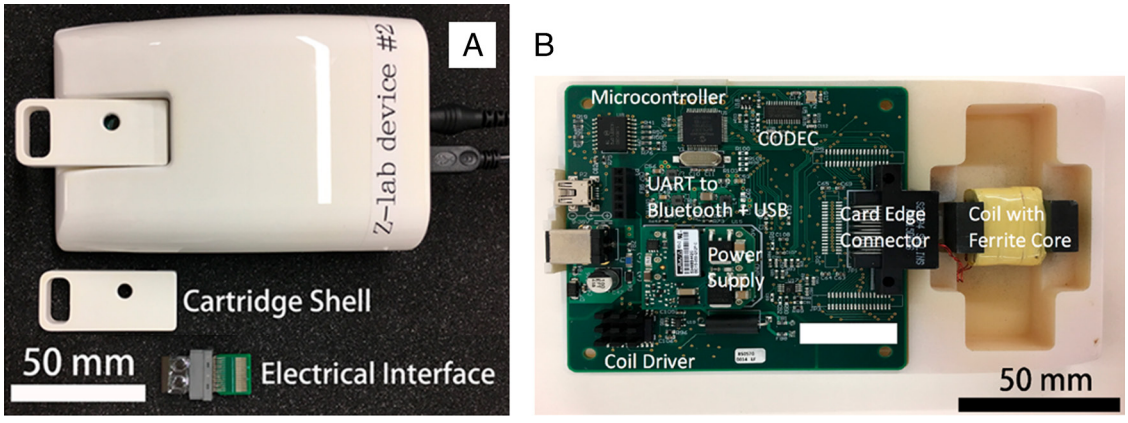

Figure 2: Picture of the GMR-based hand-held device (a), and top view of the electronic section with highlighted the main components (b) (Wu et al., 2017, 2020).

Figure 3: Picture of GMR-based portable device reported by the researchers from Stanford University (Choi et al., 2016).

sensing cartridge, and smartphone interface. The sensing cartridge consists of an 8×8 GMR sensor array. When the cartridge is placed into the reader, the electrical resistance is recorded for each sensor in real-time, and a suitable smartphone application shows the results. The reader station includes two Direct Digital Synthesis for generating sinusoidal signals to excite a Helmholtz coil and the GMR cartridge. The signal from the GMR sensor is amplified after the carrier is subtracted.

Magnetic Tunnel Junctions (MTJs) are based on stack structures similar to the GMR stacks, except that the adjacent ferromagnetic layers are separated by an insulating layer (usually an oxide). These sensors typology offers an improved MR response and higher sensitivity. However, the main issue of the MTJ sensor is its high intrinsic noise that limits the device sensitivity. Grancharov et al. (2005) reported the first-ever proof of Magnetic Tunnel Junctions (MTJs) as a biosensor. They demonstrated a unique antigen and DNA detection method at room temperature using mono-dispersed manganese ferrite nanoparticles as the magnetic tags. Li et al. (2016) propose a rapid detection system for the p24 HIV antigen in serum/plasma based on the MgO-based MTJ structure equipped with 20 nm magnetic carboxyl-group functionalized nanoparticles. In particular, the MJT array uses a sensing area equal to 890×890 μm^2 for obtaining a detection sensitivity of the p24 antigen equal to 1.39%/Oe.

Unlike the MR sensors, the MPS technology is essentially volume-based, directly detecting the dynamic magnetic responses of MNPs, thus constituting the only signal sources and indicators for probing the target analytes inside the non-magnetic media. Specifically, the MPS-based biotests exploit the nonlinear MNPs' magnetic responses and their rotational spin, as detection indicators. This platform is characterized by external sinusoidal magnetic fields (namely excitation fields), which periodically magnetize (and magnetically saturate) the MNPs. Pick-up coils capture the time-varying dipolar magnetic fields generated by MNPs as a response to the applied fields. Then, the MPS spectra are extracted and analyzed.

There are two types of MPS-based immunoassay platforms: volume and surface-based platforms. Both techniques use the dynamic magnetic responses of MNPs for assay purposes, but with different degrees of freedom. In volume-based MPS platforms, MNPs are dispersed in the liquid phase, on which external magnetic fields are applied. The MNPs immersed in the biological/chemical reagents, such as antibodies (DNA, RNA, and proteins), act as high-specificity probes to capture target analytes present in the biofluid samples. The successful recognition and binding events on MNPs produce increased hydrodynamic volume. Due to the increased hydrodynamic volume, the Brownian relaxation of the MNPs into the solution is strongly reduced, and magnetic responses are also reduced. Moreover, phase lags between the magnetic moments and external fields are increased, whereas the MPS spectra show a reduction of the harmonic amplitudes.

Orlov et al. (2016) have demonstrated a surface-based MPS platform with the lateral-flow measurement with multiplexed Lateral-Flow (LF) assay for the detection of botulinum neurotoxin (BoNT) types A, B, and E. The lateral flow method is applied using optical labels made of latex, Au, Ag, and QDs (Quantum Dots), which results in not high sensitivity. However, by replacing these optical labels with magnetic labels (i.e., MNPs), a high-sensitivity, high-stability, and low-background-noise biosensing platform is achieved. Each test strip is named A-strip, B-strip, and E-strip, for detecting BoNT-A, -B, and -E, respectively. Each strip comprises a conjugation pad, overlapping sample pad, nitrocellulose, and wicking pad, all placed on an adhesive plastic backing sheet. The anti-BoNT capture antibodies are deposited onto the nitrocellulose membrane labeled as test line and the corresponding MNP–detection antibody complexes are deposited on the conjugation pad (Figure 4).

The amplitudes of the magnetic signal recorded from the MPS are correlated with the concentration

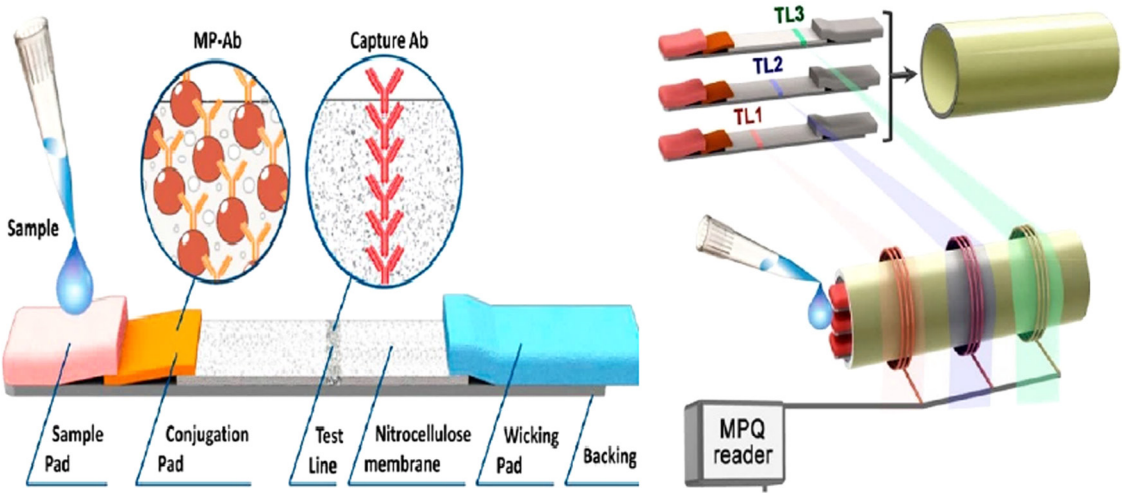

Figure 4: Test-strip design and setup (Orlov et al., 2016).

(quantity) of target analytes. Many other portable MPS immunoassay platforms have been created. For example, the platform, in ref. Pietschmann et al. (2020), is a surface-based immunoassay platform MInD (magnetic immunodetection) for the detection of SARS-CoV-2-specific antibodies. In their work, a porous polyethylene filter matrix coated with a SARS-CoV-2 spike–protein peptide acts as the reaction surface.

In another interesting work, Zhang et al. (2013) demonstrated the possibility of using a volume-based MPS bioassay method for molecular sensing applications. The MNPs are functionalized with two antithrombin DNA aptamers; the target analytes (i.e., thrombin) link MNPs together through DNA–DNA interactions, inhibiting the rotational freedom of MNPs and thus reducing the magnetic responses. They showed a LOD of 4 nM and 2 pmol for the detection of thrombin. Besides, they also demonstrated the possibility of detecting a single-strand DNA (ssDNA) in the serum with a LOD of 400 pM. This pioneering work has indicated that volume-based MPSs represent a promising platform for versatile bioassay and highly sensitive for future applications.

Another category of magnetic biosensors is the NMR platform (also called Magnetic Relaxation Switching), which employ MNPs as contrast enhancers generating an inhomogeneity of the local magnetic field and perturbing the variations of precession frequency in millions of surrounding water protons (Blümich, 2016). Nuclei, such as Hydrogen (H), Carbon (C), and Phosphor (P) featured by an odd number of protons and/or neutrons exhibit intrinsic magnetic moments and thus possess nonzero spin. Whenever an external static magnetic field, H0, is applied along the z-direction, the nuclear spin behaves like a small magnetic bar and executes precession motions about the field direction with a Larmor frequency. Upon removal of this external field, the nuclear spins are randomized, showing 0 overall magnetization. When a Radio-Frequency (RF) pulse is applied orthogonal to the static field H0, these nuclei are flipped toward the x–y plane. A tipping angle of 90° (i.e., flipping the nuclear spins to the x–y plane) can maximize the resultant NMR signal in the transverse plane. When the RF pulse is removed, these nuclei relax back to equilibrium states. The RF coils monitor the transverse and longitudinal magnetizations of these nuclear spins, by measuring the related magnetic fluxes. The longitudinal relaxation time T1 is the time taken by the z component of the nuclear spin (magnetization) to come back to its thermal equilibrium value, whereas the transverse relaxation time T2 is the measure of the decay of net magnetization in the x–y plane (perpendicular to H0). The reciprocals of T1 and T2 indicated as R1 and R2, are the longitudinal and transverse relaxation rates.

In most applications, the NMR technique detects the MNP-labeled targets by measuring the precessional signal of the H proton into the entire sample volume (Orlov et al., 2016). In this way, the NMR platform can be classified as a volume-based immune assay method.

In recent years, there have been many advances in miniaturizing the NMR platforms such as assembling electronics into integrated-circuit chips, implementing smaller or planar NMR coils and compact permanent magnets, and mounting microfluidic channels (Hale

et al., 2018; Jeyaprakash and Mukesh, 2015; Smits et al., 2019). These low-cost micro NMR platforms (μNMR) have demonstrated portability, robustness, versatility, and even higher sensitivity than conventional systems. With these capabilities, it is expected that an NMR hand-held device can be an essential tool for personal care and accurate diagnostics for infectious diseases in rural areas and mitigates the healthcare burden.

For example, Lei et al. (2015) presented a portable miniaturized micro-nuclear magnetic resonance relaxometer for automated multi-sample chemical/biological analysis. The system integrates a small Tesla magnet for carrying out the NMR assay on biological samples probed by MNPs; the relaxation time is determined using multiplexed μNMR sampling. An integrated transceiver converts the magnetic signal, captured by the embedded coils, into an electric signal by analyzing sub-10 μL samples. Carried out tests demonstrate that designed μNMR and employing biotinylated Iron NPs, 0.2 μM sensitivity is reached. The advantages and disadvantages (without the assay sensitivity) of the afore-described platform are summarized and compared in Table 1.

Furthermore, each platform's assay specificity depends on external factors such as the antibody typologies and the assay modalities; for this reason, the assay specificity of each platform is not listed or compared in Table 1.

In general, magnetic nano-sensors' platforms are featured by easier sample preparation than standard optical techniques; they use safer magnetic labels

Table 1. Advantages and disadvantages of different magnetic nano-sensors technologies (Wu et al., 2020).

Platform	Advantages	Disadvantages
GMR	High sensitivity	Multiple washing steps usually required, thus needing well-trained technicians, but can be wash-free, which reduces the sensitivity
	Availability of a portable device	Time-consuming
	Mass production capability	High cost per test; nanofabrication of GMR biosensors required
MTJ	High sensitivity	Multiple washing steps usually required, thus needing well-trained technicians, but can be wash-free, which reduces the sensitivity
	Mass production capability	High noise; large distance from the MNP to the sensor surface
		Hard-to-acquire linear response
		Complicated fabrication process
		Time-consuming
		High cost per test; nanofabrication of MTJ biosensors required
MPS, surface-based	High sensitivity	Multiple washing steps usually required, thus needing well-trained technicians, but can be wash-free, which reduces the sensitivity
	Low cost per test	Time-consuming
	Availability of a portable device	
MPS, volume-based	One-step wash-free detection allowed	Medium sensitivity
	Immunoassays that can be hand-held by non-technicians	
	Low cost per test	
	Availability of a portable device	
NMR	Availability of a portable device	Multiple washing steps usually required, thus needing well-trained technicians, but can be wash-free, which reduces the sensitivity
		Time-consuming
		Medium sensitivity

than electrochemical techniques and produce more homogeneous detection than mechanical methods. Given these advantages, we expect them to replace or supplement the current diagnosis techniques that rely on non-magnetic strategies. This paradigm shift could contribute to better surveillance and control of SARS-CoV-2 infection in populations.

Zhao et al. (2021) developed an ultrasensitive electrochemical technology based on functionalized graphene oxide for detecting the SARS-CoV-2 virus. Given that COVID-19 patients have no specific symptoms, SARS-CoV-2 detection is indispensable for an accurate diagnosis. Although the antibody-based serological tests are convenient and rapid, the technological issues limit their applicability. Since these tests require to check the antibodies produced by the human organism against SARS-CoV-2 following symptom onset, they take a substantial amount of time. Moreover, SARS-CoV-2 antibodies have significant cross-reactivity with the antibodies generated by other coronaviruses. For this reason, nucleic acid-based real-time reverse transcription Polymerase Chain Reaction (PCR) (RT-qPCR) assays are worldwide employed for the virus RNA detection. However, RT-qPCR has some drawbacks since it requires expensive instruments and reagents, the need for trained personnel, and sometimes RT-qPCR detection kits produce false-negative results (Afzal, 2020).

Electrochemical biosensors represent an alternative solution due to their advantages, such as low cost, high sensitivity, user-friendliness, and robustness. Among the nucleic acid biosensors, a super-sandwich-type electrochemical biosensor has attracted a lot of attention for its high specificity and sensitivity. This biosensor is composed of a Capture Probe (CP), Label Probe (LP), Target Sequence, and Auxiliary Probe (AP). The 5- and 3-terminals of the target sequence are complementary to CP and LP, respectively, and the 5- and 3- regions of AP have complementary sequences with two different LP areas. The sequence-specific detection can be obtained using CP and LP, and AP hybridizes many times with LP to produce long concatamers, resulting in higher sensitivity. The sensitivity can be enhanced by facilitating the LP with signal molecules through other molecules or materials. In this study, the authors developed a super-sandwich-type electrochemical biosensor based on p-sulfocalix arene (SCX8) functionalized graphene (SCX8-RGO) to enrich TB for COVID-19 RNA detection through the following procedures:

- The CPs labeled with thiol were immobilized on the surfaces of the Au@Fe3O4 nanoparticles and formed CP/Au@Fe3O4 nanocomposites;
- The host-guest complexes (SCX8-TB) were immobilized on RGO to form Au@SCX8-TB-RGO-LP bioconjugate;
- The sandwich structure of 'CPtarget-LP' produced; and
- AP was introduced to create long concatamers, as shown in Figure 5.

They developed a plug-and-play method to achieve an accurate, sensitive, and rapid detection of SARS-CoV-2 samples from various clinical specimens without RNA amplification, by using an electrochemical biosensor equipped with a smartphone, providing a simple and low-cost method for point-of-care testing (POCT) (Figure 5).

Primer pairs were synthesized by the sequences provided by the Chinese Center for Disease Control and Prevention (CDC) and used to amplify the ORF1ab gene in real-time PCR (qPCR). In specificity characterization, they aligned the genomes of SARS-CoV-2 through the BLAST analysis of NCBI COVID resources, so a high conservation region was selected.

Then, the authors prepared A and B premixes (as shown in Figure 5) to detect SARS-CoV-2; afterward, they prepare detection samples by including artificial

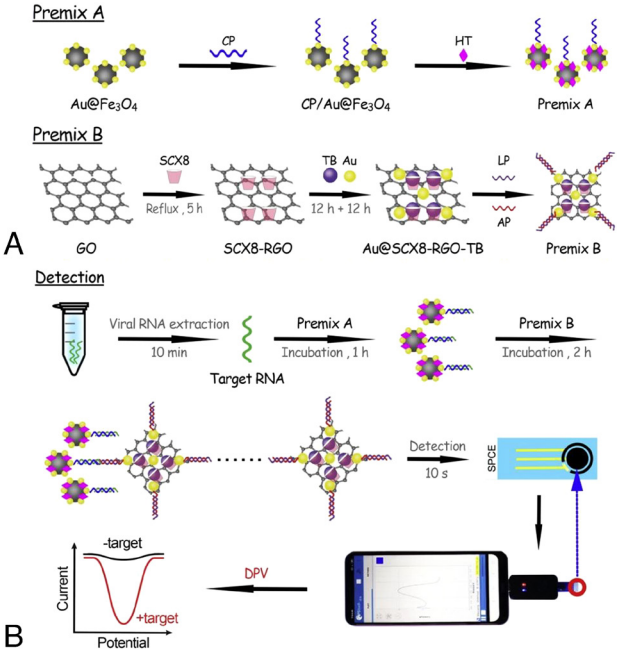

Figure 5: Schematic representation of SARS-CoV-2 detection using the electrochemical biosensor. (a) Prepare the premix A and B; (b) Process of electrochemical detection using a smartphone (Zhao et al., 2021).

targets and clinical RNA samples. Since the RNA is easy to degrade, they synthesized the corresponding target sequences of ssDNA according to the published RNA sequences of SARS-CoV-2 for electrochemical detection. All the clinical samples used in this study were collected from the Second People's Hospital of Yunnan Province. In particular, a total of 88 samples from 25 confirmed patients and eight patients infected by SARS-CoV-2 were considered and inactivated by heating them at 56°C for 30 min. All RNAs were extracted using a Tianlong DNA/RNA virus mini-kit, and the prepared samples were stored at −80°C before use.

Subsequently, they made electrochemical and RT-qPCR measurements (using a commercial 2019-nCOV ORF1ab/N nucleic acid detection kit). They discovered that a *p*-value lower than 0.05 was statistically significant and indicated that the sample is positive. Later, the authors analyzed the characterization of nanocomposites, and all the results displayed the successful preparation of the RGO-SCX8-Au nanocomposites. RT-qPCR results highlighted that 35 of 62 specimens were positive from the confirmed patients (56.5%), and two of 26 samples from the hospitalized patients (7.7%) were present. Therefore, the detectable positive rate was equal to 85.5%, thus demonstrating that the electrochemical test is more sensitive than the RT-qPCR assay for SARS-CoV-2 detection. Also note that, compared to the RT-qPCR assay, the developed SARS-CoV-2 biosensor was superior to other assays in detecting upper respiratory samples.

The proposed SARS-CoV-2 biosensor presented high sensitivity and specificity thanks to the following factors:

- The use of the super-sandwich-type electrochemical biosensor improve the specificity and increased signal enrichment ability;
- Many nanomaterials of high conductivity promote the signal intensity; and
- Super-molecular recognition plays an important role in the enrichment of molecule TB for improving the sensitivity of the biosensor.

To ensure detection accuracy, they initially performed homology analyses of their designed CP sequences targeting SARS-CoV-2 in silicon. After the alignment of 2,291 complete genomes of SARS-CoV-2 obtained from the GenBank databases, the results showed that the SARS-CoV-2 RNA sequences binding to CP were completely conserved (100%).

Vadlamani et al. (2020) reported the synthesis of a cheap and highly sensitive electrochemical sensor based on cobalt-functionalized TiO_2 nanotubes (Co-TNTs) for quick detection of SARS-CoV-2 through sensing the spike protein (receptor-binding domain (RBD)) present on the surface of the virus. A low-cost and straightforward electrochemical anodizing technique was used for synthesizing TNTs, followed by an incipient wetting method for cobalt functionalization of the TNTs, then connected to a potentiostat for the signal collection. This sensor detects the S-RBD protein of SARS-CoV-2 even at very low concentration (ranged from 14 to 1,400 nM (nanomolar)) featured by a linear response in detecting viral protein within the concentration range. Thus, their Co-TNT sensor is very effective in detecting SARS-CoV-2 S-RBD protein, approximately in 30 s.

The main issues of the actual diagnostic tests are their invasive nature, requiring trained personal for nasopharyngeal sample collection, along with the requirement of highly sophisticated machines, cross-reactivity with other viruses, and a longer duration of testing. Electrochemical biosensors are based on electrode material and form factor, and widely used for virus detection based on aptamers, antibodies, and imprinted polymers. Also, these sensors have the advantage of being sensitive to biomolecules due to their ability to detect biomarkers with specificity, accuracy, and high sensitivity. Electrochemical biosensors have already been successfully used in medical diagnostics for the detection of other viruses, like the Middle East respiratory syndrome coronavirus (MERS-CoV), the human influenza A virus H9N2, the human enterovirus 71 (EV71), and the avian influenza virus (AIV) H5N1. Electrochemical biosensor operation can be improved by nano-structuring the electrode, increasing the electrochemical reaction rate thanks to the larger electrode surface area to volume ratio, and in this way, the electrode surface area exposed to the analyte fluid volume.

Chin et al. (2017) proposed a detection mechanism based on the formation, upon the nanostructured carbon electrodes, of a complex between Cobalt (Co) and the biomarker at a specific bias voltage, because of the reduction of Co ions oxidation of the biomarker. Similarly, the SARS-CoV-2 can be detected through complexing of functionalized nanoparticles with the S-RBD protein (Figure 6) (Vadlamani et al., 2020).

The data show that cobalt functionalized TNTs can selectively detect the S-RBD protein of COVID-19 using the amperometry electrochemical technique. At first, the TNTs were synthesized by electrochemical anodization of the Ti sheet. Afterward, this was cut out of a G1 grade Ti sheet (thickness ~10 µm), and one side was polished to remove any surface metal oxide layer. The coupon was ultrasonicated, and the unpolished side was masked with Kapton tape to

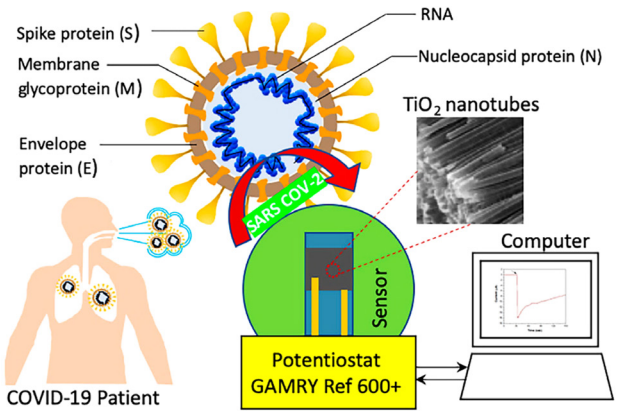

Figure 6: Schematic of Co-functionalized TiO2 nanotube (Co-TNT)-based sensing platform for detecting SARS-CoV-2 (Vadlamani et al., 2020).

prevent any exposure to electrolyte during anodization. Therefore, the electrochemical anodization was performed in a standard two-electrode configuration, and then, the anodization carried out. The sample was rinsed, and the Kapton tape was removed from sample after baking; finally, it was cooked again in a tube furnace at 500°C for 3 h.

The annealed TNTs were functionalized with cobalt using an incipient wetting method; then, the same side of the sample was masked again with Kapton tape and ultrasonicated for 35 min. Therefore, the sample was baked in an oven at 120°C for 4 h to obtain the cobalt functionalized TNTs. By SEM imaging, the morphology of the TNTs and Co-TNTs were examined and analyzed using the ImageJ software. The pCAGGS vector containing SARS-CoV-2 Wuhan-Hu-1 spike glycoprotein RBD was obtained from BEI Resources (National Institute of Allergy and Infectious Diseases-NIAID, National Institute of Health-NIH, NR-52309). The HEK293T cells were grown at 37°C in a humidified chamber and then transfected by recombinant plasmid for the His6-tagged S-RBD protein generation. The supernatants from transfected cells were, then, incubated with 1 mL of nickel-nitrilotriacetic acid (Ni-NTA) Agarose (Qiagen) for every 10 mL of supernatant, for 2 h at 4°C with rotation. The eluted protein was concentrated using protein concentrators, quantified using Bradford assay and Nanodrop (produced by ThermoFisher Scientific), and further analyzed by Sodium Dodecyl Sulphate – PolyAcrylamide Gel Electrophoresis (SDS-PAGE).

The electrochemical sensing of S-RBD protein was carried out using a custom-built Co-TNT packaged on a printed circuit board, consisting of a clamp for holding the Co-TNT grown over the Ti sheet. The upward-facing Co-TNT side acts as a working electrode; vice-versa, the bottom-facing Ti side acts as a counter electrode.

From SEM images of Figure 7, the outer diameter and the wall thickness of TNTs were 60 and 10 nm, respectively, as well as the average length of TNTs was equal to about 1.1 µm. The surface morphology of the Co-TNT was examined, revealing the presence of precipitates on top of the TNT surface, as well as also Ehlers–Danlos syndrome (EDS) analysis confirmed the uniform distribution of Co ion on top of TNTs. The RBD of the spike glycoprotein (S-RBD), also comprising amino acids 329–521, is an easily accessible target for the detection of SARS-CoV-2. The ability of Co-TNT to detect the S-RBD protein of SARS-CoV-2 was determined by performing an amperometry experiment using a bias voltage of –0.8 V. The sensor was exposed to protein for 30 s after the beginning of the experiment. The sensor response increases rapidly, due to the electrochemically triggered protein unfolding and subsequent formation of the complex between Co and the protein. The average sensor response time, defined as the time taken to reach the peak current, was found to be 2 s.

The sensor response (SR) was calculated with the equation:

$$Sensor\ Resposne\ (SR) = \frac{\left(i_{max,protein} - i_{max,base\ line}\right)}{i_{max,base\ line}}$$

where $i_{max,\,base\ line}$ is the maximum current obtained when the sensor is not exposed to the protein. The sensor response increased with the concentration of protein and the LOD can be improved using (i) Co-TNT synthesized by an in-situ anodization technique and (ii) Co-TNTs with higher length. The higher sensor sensitivity obtained by using longer Co-TNTs results in a more significant reaction rate; lastly, a higher sensor response can be obtained even at lower protein concentrations.

Samson et al. (2020) provide an overview of new biosensors used to detect RNA-viruses, including nucleic-acid sensors, CRISPR-Cas9 paper strip sensors, antigen-Au/Ag nanoparticles-based electrochemical biosensors, aptamer-based bio-nanogate, surface plasmon resonance (SPR) sensor, and finally optical biosensor. These technologies could be useful tools for accurate, rapid, and portable diagnosis in the current pandemic that has affected the world. The sensor response is mediated by IgM

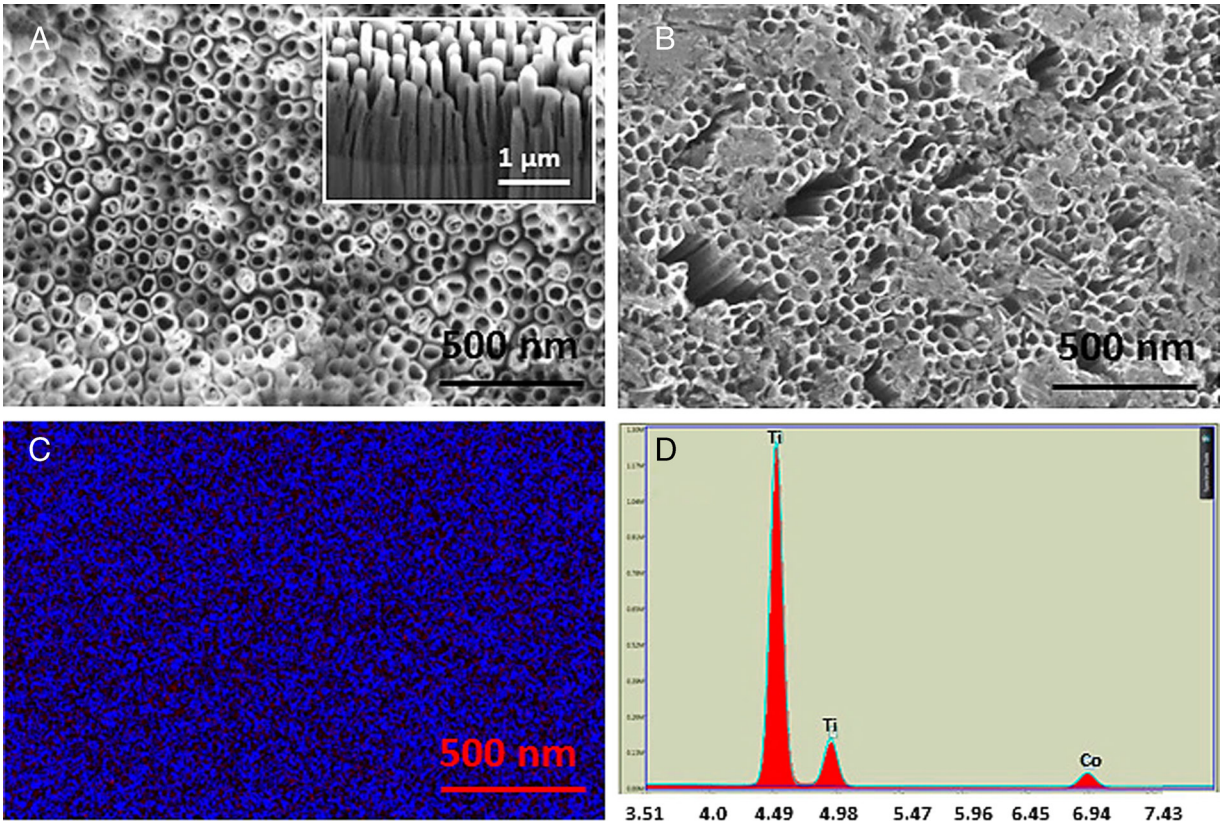

Figure 7: Scanning electron microscopy (SEM) micrographs of (a) TiO2 nanotubes (TNTs) post-annealing. Inset shows sidewalls of TNTs, (b) Co-functionalized TNTs showing the Co (OH)2 precipitate, (c) EDS map of Co confirming its uniform distribution, and (d) EDS spectra confirming the presence of Co (Vadlamani et al., 2020).

and IgG antibodies, used to detect the COVID-19 disease and used for its possible therapy, known as plasma therapy. To bypass the limitations of qRT-PCR based assay, a highly specific RT-LAMP (Reverse Transcription Loop-Mediated Isothermal Amplification) assay method is available for detection of SARS-CoV-2 (Park et al., 2020; Yu et al., 2020; Zhou et al., 2020).

Moreover, the use of modern gene-editing CRISPR-Cas (Clustered Regularly Interspaced Short Palindromic Repeats) systems was proposed to detect the virus, as reported in (Zuo et al., 2017). This technique can also detect microRNAs, bacteria, and cancer mutations, simply changing the target-specific crRNA/sgRNA. The gene-editing technique was applied to a biological sensor-based CRISPR-Chip paired with a graphene-based field effect transistor (FET) to detect up to a 1.7 fM quantity of nucleic acid without the necessity for amplification and within a short span of 15 min (Hajian et al., 2019). The FET-based biosensing devices employ the coating of the graphene sheets of the FET with a monoclonal antibody against the SARS-CoV-2 spike protein (Figure 8).

The authors have determined the sensor sensitivity using antigen protein, cultured virus, and nasopharyngeal swab specimen provided by

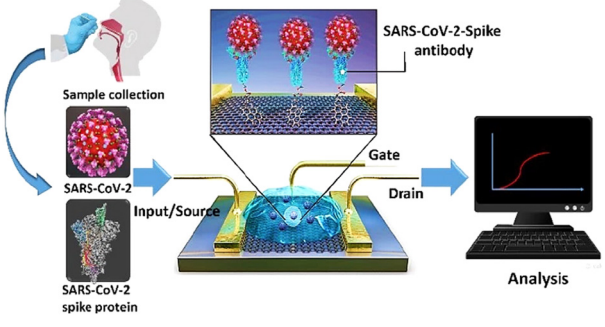

Figure 8: Schematic diagram of COVID-19 FET-based biosensor operation (Seo et al., 2020).

COVID-19 patients. This FET biosensor can detect 1 fg/mL concentration of SARS-CoV-2 protein in phosphate-buffered saline (PBS) and 100 fg/mL concentration in the clinical transport solution.

Recently Mahari et al. (2020) developed a home-made biosensor device (named eCovSens) fabricated with fluorine-doped tin oxide (FTO) electrode together with gold nanoparticles (AuNPs) and nCOVID-19 antibody (Figure 9). This last was compared with a commercial potentiostat machine used to detect an nCOVID-19 spiked protein antigen (nCOVID-19 Ag) in the saliva samples. A potentiostat sensor was fabricated using FTO electrode enriched with gold nanoparticles (AuNPs) and immobilized with nCOVID-19 monoclonal antibodies (nCOVID-19 Ab) to measure the changes of electrical conductivity.

Likewise, eCovSens was used to measure changes in electrical conductivity through immobilizing nCOVID-19 Ab on a screen-printed carbon electrode (SPCE). The performances of sensors were recorded after the interaction of nCOVID-19 Ab with an nCOVID-19 specimen. The FTO-based immune-sensor and the proposed SPCE-based biosensor device reported high sensitivity for early detection of nCOVID-19 Ag, ranging from 1 fM to 1 µM (under optimum conditions). Furthermore, the authors demonstrated that the eCovSens device was able to successfully detect nCOVID-19 Ag with a concentration of 10 fM in a standard buffer. In particular, the LOD was 90 fM with eCovSens and 120 fM with a potentiostat, in the case of saliva specimens. The proposed portable point of care (PoC) can be used for the rapid detection of nCOVID-19 since a 10–30 s detection time is ensured.

The DNA capturing sequence was immobilized on the silk-screened electrode surface and hybridized with biotinylated target strand DNA. This strategy could be useful for detecting the SARS-CoV-2 virus to change the immobilized thiolated nucleic acid sequence. This technique is capable of detecting a 4.7 nM concentration of complementary nucleic acids.

Another electrochemical and paper-based biosensor was used to detect the chikungunya virus (Zuo et al., 2017). These paper-based biosensors used the ultra-high charge-transfer efficiency of AuNPs associated with the magnetic NPs (Fe_2O_4). This electrochemical biosensor is simple, biodegradable, and economical. In this scenario, another novelty concerns a novel DNA hydrogel formation by isothermal amplification of the complementary target (DhITACT-TR) system, which has been successfully used to detect the MERS (Middle East Respiratory Syndrome) virus. This methodology is featured by high sensitivity, rapid detection time and easy use since the result, based on fluorescent emission, can be diagnosed by the naked eye (Figure 10) (Jung et al., 2016).

In conclusion, traditional techniques, like PCR and sequencing, are time-consuming, and might not fulfil the new challenges (such as rapid mutations) and demands (for mass populations) for the faster and direct detection of viral pathogens.

Mauriz (2020) explored the recent progress of the plasmonic nanostructures applications for virus detection, which has lately gained great attention, due to their versatility, low time of response, and label-free

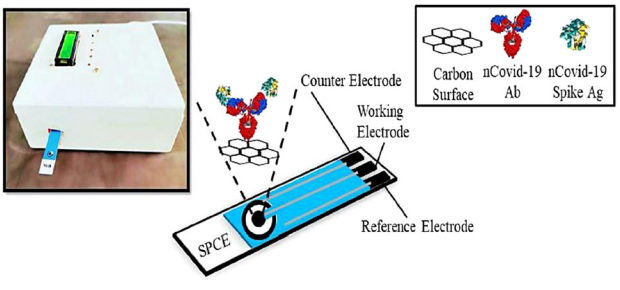

Figure 9: Graphical representation of the working operation of the eCovSens device using SPCE electrode, including COVID-19 antibody (Mahari et al., 2020).

Figure 10: DhITACT-TR chip for robust detection of target pathogen in a single-step injection of RNA extract (Samson et al., 2020).

monitoring. Also, their potential for multiplexing and system miniaturization are additional benefits for PoC testing. These features, along with the possibility of taking advantage of nanomaterials' electronic and physical properties, have allowed the creation of smaller and ultrasensitive detection frameworks. Therefore, nanoplasmonic biosensors seem to represent an excellent approach to ensure ultra-low detection limits of viral particles, antigens, or nucleic acids from clinical samples (i.e., blood, serum, saliva, etc.). Most of the plasmonic applications for virus sensing rely on the well-known operation principles of SPR, but, to obtain optimal performance, new design strategies are required to maintain the sensitivity and specificity of measurements, as well as preserving the biocompatibility of the immobilized biological receptor. These plasmonic biosensors exploit propagation of surface plasmons along with the interface of a thin metal layer (commonly noble metal), and a dielectric (aqueous medium).

In other terms, the plasmonic biosensor takes advantage of the local refractive index changes of the transducer surface during the monitoring of the molecular interactions among the target analyte and the immobilized biological receptor. The binding events occurring on the surface can be monitored in two different forms: SPR and localized surface plasmon resonance (LSPR), both functions of the surface refractive index. However, the dimension of the plasmonic nanomaterial is very important for determining the difference between SPR (based on thin metallic layers) and LSPR approaches. In particular, the latter is featured by dimensions lower than the incident wavelength (Figure 11).

This characteristic allows controlling the spatial resolution of LSPR configurations by designing the geometry and composition of metallic nanostructures. The local electromagnetic field can optimize the optical processes such as the fluorescence and Raman scattering, leading to Surface-enhanced Raman Scattering and plasmon-enhanced electrochemiluminescence sensing schemes. The sensitivity, achieved by both the optical configurations, is higher than those of both SPR and LSPR.

For example, a new approach combines the effect of plasmonic photothermal (PPT) and LSPR sensing, to detect DNA-selected sequences via the hybridization of DNA receptors immobilized on two-dimensional gold nano-islands (AuNIs). This plasmonic dual-functional biosensor takes advantage of the PPT heat generated on the AuNIs' chip to increase the hybridization temperature and discriminate two similar gene sequences (RNA-dependent RNA polymerase RdRp genes) from

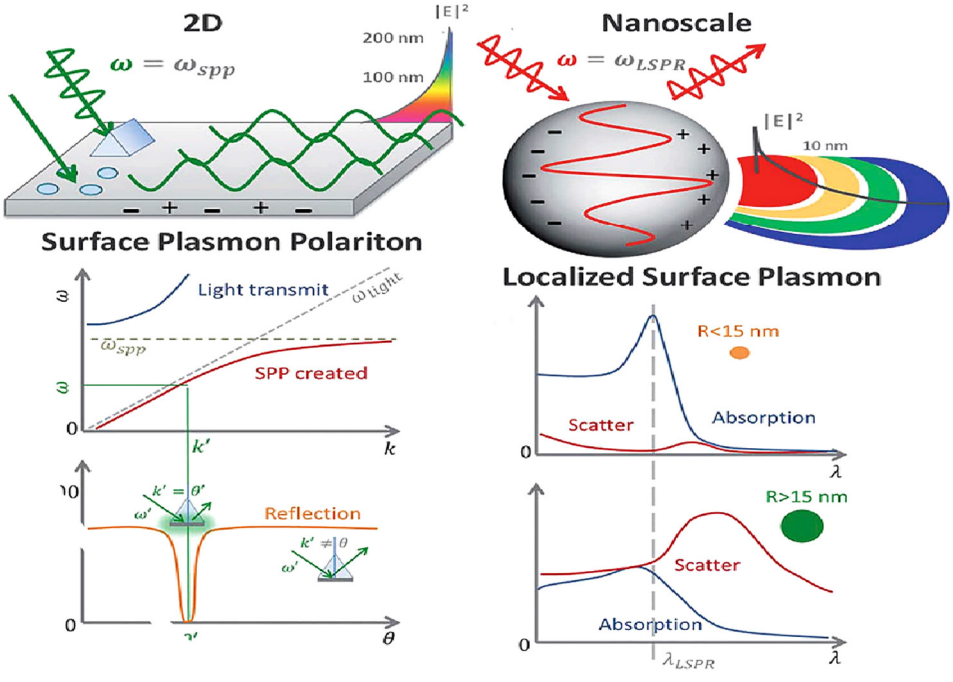

Figure 11: The surface plasmon polariton (SPP) can only be excited at specific wave vectors and decays evanescently from the surface. The momentum-matching condition leads to the SPP resonance and only exists at certain incident angles (Li et al., 2015).

SARS-CoV and SARS-CoV-2. A detection limit of 0.22 pM was obtained using a multigene mixture including DNA sequences of the RdRp-COVID, an open reading frame 1ab (ORF1ab)-COVID nucleic acid, and E genes from SARS-CoV-2.

Another innovative approach for COVID-19 detection is the colorimetric assay. This approach is based on gold nanoparticles (AuNPs), functionalized with thiol-modified antisense oligonucleotides (ASOs) specific for N-gene (nucleocapsid phosphoprotein) of SARS-CoV-2 (Moitra et al., 2020). The biosensing scheme comprised the change of its SPR absorbance spectra with a redshift of ~40 nm when thiol-modified AuNPs agglomerates selectively with their target RNA sequence. This application demonstrated that the addition of endonuclease Ribonuclease (RNAse H) brings to a visually detectable colorimetric change thanks to the aggregation with the AuNPs. The assay selectivity was tested in the presence of MERS-CoV viral RNA, showing a LOD of 0.18 ng μL^{-1} of RNA with SARS-CoV-2 viral load. The principal advantage of the proposed method is its capability to target other regions of viral genomic material, such as E-gene (envelope protein), S-gene (surface glycoprotein), and M-gene (membrane glycoprotein) without using sophisticated instrumental techniques.

IoT solutions and systems for monitoring and limiting the COVID-19 pandemic spreading

COVID-19 has pushed the scientific community around the world to create, improve, and communicate heterogeneous systems to minimize the virus's impact on our lives. This paragraph explored the new technologies for monitoring, detecting, and containing the spreading of COVID-19 pandemic. In particular, we have investigated the Internet of Things (IoT) solutions for early detecting the onset of the infection symptoms, such as fever and breathing problems (Figure 12).

Otoom et al. (2020) proposed a real-time COVID-19 tracking and detection system that uses an IoT architecture for collecting real-time symptoms data from infected users (Hernández and Sallis, 2020; Jung, 2020) and for the following aims (Figure 13).

- Rapidly identifying suspected coronaviruses cases,
- Monitoring the response to the treatment of infected patients, and
- Understanding the symptoms of the virus by collecting and analyzing relevant data.

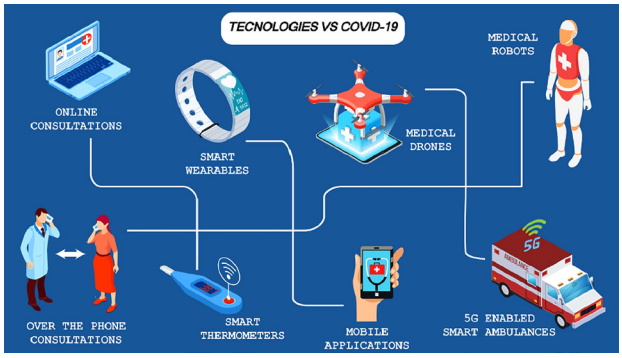

Figure 12: Different technologies versus the COVID-19 (Chamola et al., 2020).

The framework consists of these five sections:

1. Symptom Data Collection and Transfer section (using wearable devices),
2. Quarantine/Isolation Center,
3. Data Analysis Section, based on machine learning (ML) algorithms,
4. Health Physicians Section, and
5. Cloud Infrastructure.

We know that the most relevant COVID-19 symptoms are as follows: fever, cough, fatigue, sore throat, and shortness of breath. To rapidly identify the potential coronavirus cases from the real-time data

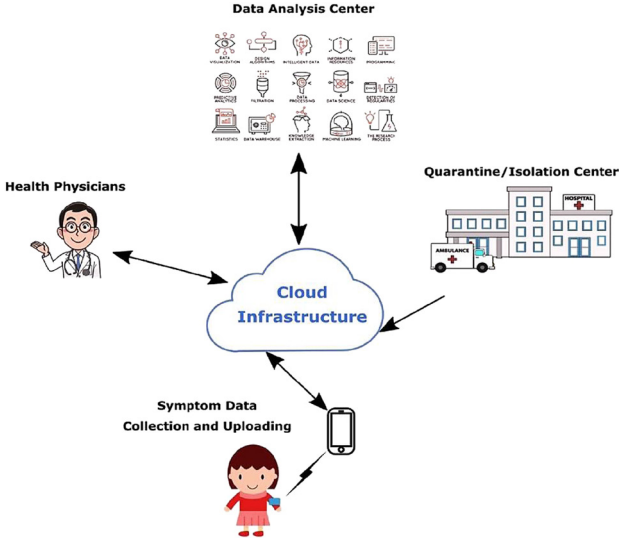

Figure 13: Representation of IoT-based framework for early identification and monitoring of new cases of COVID-19 virus infections (Otoom et al., 2020).

collected, the use of eight ML algorithms, namely Support Vector Machine (SVM), Neural Network, K-Nearest Neighbor (K-NN), Naïve Bayes, Decision Stump, Decision Table, ZeroR, and OneR is proposed. The system in question could be implemented with an IoT infrastructure to monitor both potentials and confirmed cases. In addition to the real-time monitoring function, this system can contribute to understanding the virus nature by collecting, analyzing, and archiving the critical data.

Among the framework components, there is also the Quarantine/Isolation Center; this component records data from users who have been quarantined or isolated in a health care centre. These records include health (or technical) data, which refer to the symptoms mentioned above, and non-technical data related to travel and contact history during the past 3–4 weeks, chronic diseases, gender, age, and other relevant information, such as the family history of illness. Another essential component is the Data Analysis Center; it hosts data analysis and ML algorithms used to build a model for COVID-19 and provide a real-time dashboard of the processed data. The model can also predict the patient treatment response. In addition , by the proposed ML-based identification/prediction mode, physicians will be able to monitor suspected cases whose real-time uploaded symptom data should indicate a possible infection.

The last component is the Cloud Infrastructure, interconnected through the internet, for uploading real-time symptom data from each user, maintaining personal health records, communicating prediction results, sharing physician recommendations, and providing information to be stored. The results showed that all ML algorithms used in this work, except the Decision Stump, ZeroR, and OneR, achieved accuracies above 90%; thus, the best algorithms would provide an effective and accurate identification of COVID-19 cases.

Maghded et al. (2020) described various developed techniques to detect the initial symptoms of the COVID-19 virus, such as medical detection kits. In this work, a new framework is described to detect the virus using the built-in smartphone sensors and predict the gravity grade of pneumonia to predict the disease outcomes. Modern smartphones integrate numerous sensors with powerful computation capabilities, allowing them to sense information about daily activities and even capture visual data. Since each symptom has its danger level different from other diseases, the framework tries to discover each symptom's level based on the built-in sensors measurements (Figure 14).

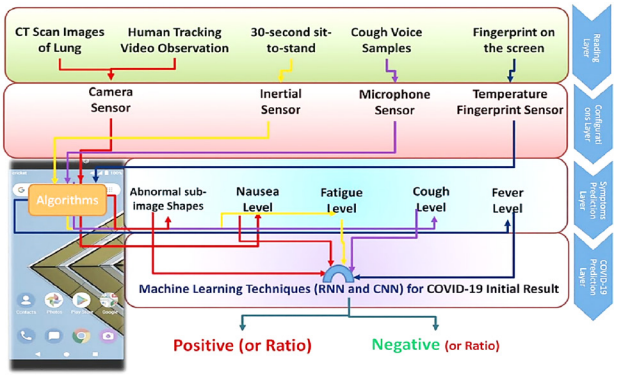

Figure 14: Scheme of the proposed framework to predict COVID-19 (Maghded et al., 2020).

The proposed framework integrates the data, acquired by sensors installed on recent smartphones, with algorithms in a single solution, deriving a predicted level of symptoms and storing them in a dataset as a single record. Therefore, such records from different patients are collected and used as input to a ML algorithm. The authors proposed a framework that consists of a set of layers. The first one is responsible for gathering data from sensors: reading the captured computed tomography (CT) scan images of lung acquired by the smartphone camera; getting the inertial sensors (accelerometer sensor) data over 30-second sit-to-stand; recording microphone voice for a series of cough; finally measuring the temperature during fingerprint touching on the smartphone screen.

The second layer configures the onboard smartphone sensors, including image size, reading intervals, timer resolution, buffers' size, etc. Afterward, the readings and configurations are used to input the symptoms algorithms running on the smartphone application. The third layer of the framework calculates the danger levels of symptoms separately and then stored them as a record input to the next layer. Meanwhile, according to the nature of recorded data, the last layer applies ML techniques to detect the COVID-19. In addition, to improve the proposed framework and get a reliable prediction result, the recorded information and the results from different users or patients are shared in the cloud; thereby, a large data set is obtained. Such a process will also provide transfer learning from multiple smartphones and various onboard sensors to new smartphones (Figure 15).

In conclusion, the proposed framework is implemented in a mobile app to verify the acquisition functions of COVID-19 symptoms used in the diagnosis

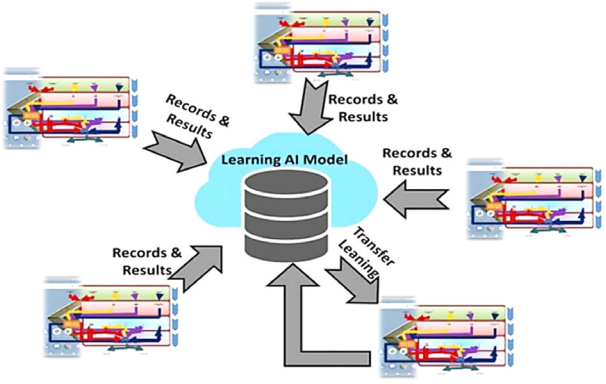

Figure 15: Cloud computing for the proposed framework (Maghded et al., 2020).

process. Figure 16 shows two screenshots related to the registration page and the transfer of the acquired data to the cloud platform.

Sun et al. (2020) analyzed the data through the smartphones and wearable devices on 1062 participants recruited in Italy, Spain, Denmark, UK, and the Netherlands. Daily, they derived nine functions, including time spent at home, maximum distance traveled from the user residence, the maximum number of Bluetooth-enabled nearby devices (as a proxy for physical distancing), step count, average heart rate, sleep duration, bedtime, phone unlock duration, and social app use duration.

As expected, following the respective national lockdowns and consequently the severe penalties for violating the imposed protocols, people stayed home longer, so people made connections with fewer Bluetooth devices nearby. Table 2 shows a complete list of features: location data derived from the smartphone was sampled once every 5 min, with longer sampling durations depending on network connectivity. Spurious location coordinates were identified and removed if they differed by more than five degrees from preceding and following coordinates (Table 2). Through the Kruskal–Wallis tests followed by posthoc Dunn's tests, the authors examined changes in mobility, functional measures, phone usage induced by the lockdowns, and the comparisons among baseline pre and during the lockdown on the daily median of each feature. These quantities were also analyzed by differentiating them by age, sex, body mass index, and educational background. The RADAR-Base open-source mHealth platform managed the data collection and manipulation. This last is an open-source platform that supports the collection and analysis of mobile and telephone data in real-time, so allowing immediate intervention.

Given the streaming nature of the platform, it is easy to provide insights into the data in real-time,

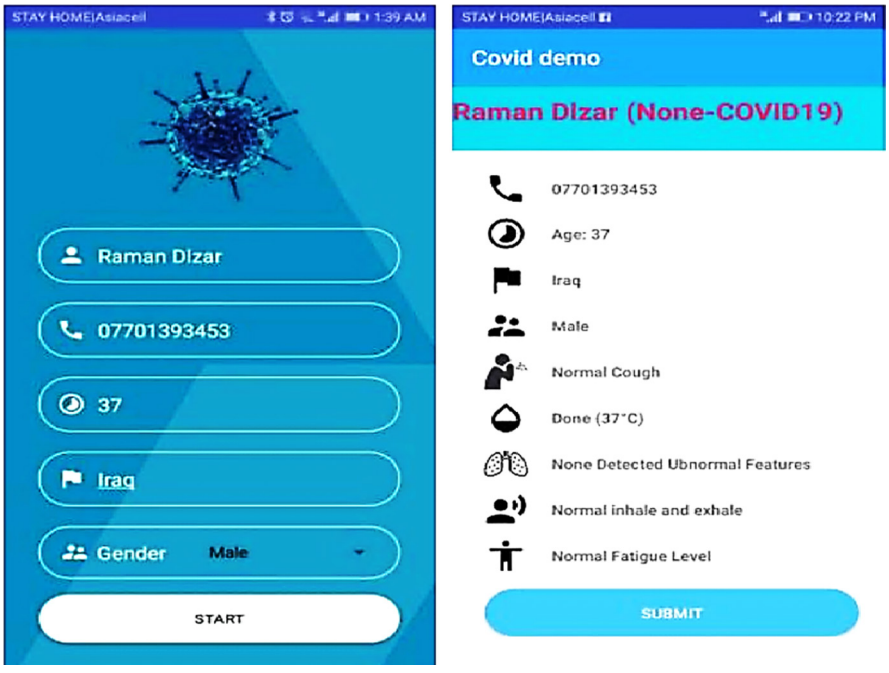

Figure 16: User registration & results of the test (Maghded et al., 2020).

Table 2. A full list of extracted features (Sun et al., 2020).

Category	Modality	Features	Extraction
Mobility	Smartphone location	Homestay	The time spent within 200m radius of home location (determined using DBSCAN)
		Maximum traveled distance from home	The maximum distance traveled from home location
	Smartphone Bluetooth	Maximum number of nearby devices	The maximum number of Bluetooth-enabled nearby devices
	Fitbit step count	Step count	Daily total of Fitbit step count
Functional measures	Fitbit sleep	Sleep duration	Daily total duration of sleep categories (light, deep, and rem)
		Bedtime	The first sleep category of the night
	Fitbit heart rate	Average heart rate	The daily average heart rate
Phone usage	Smartphone user interaction	Unlock duration	The total duration of phone in the unlocked state
	Smartphone usage event	Social app use duration	The total duration spent on social apps (Google Play categories of Social, Communication, and Dating)

thus making the results potentially usable for localized monitoring. In fact, through RADAR-based measures, they quantified changes in mobility, phone use, and functional measures as a result of non-pharmaceutical interventions introduced to control COVID-19 diffusion. Finally, the RADAR-based system has proven itself capable of collecting data from wearables and mobile devices to determine the health system's responsiveness against the COVID-19 outbreaks. This capacity to monitor the reactions to interventions in real-time is essential to understand the behavior of the COVID19 disease.

Nasajpour et al. (2020) have examined the role of IoT-based technologies in COVID-19 and reviewed the state-of-the-art architectures, platforms, applications, and industrial IoT-based solutions for combating COVID-19 in three main phases, including early diagnosis, quarantine time, and after recovery. During this pandemic, wearable devices are an efficient way to respond to the need for early diagnosis. For example, a wide range of IoT smart thermometers has been developed to record the patients' body temperature continuously because the use of these should decrease the spread of the virus as it is not necessary for health workers to be in close contact with patients (which happens using the old types of thermometers). These low-cost, accurate, and easy-to-use devices could be worn or stuck to the skin under clothing. Other smart thermometers can report body temperature at any time on a smartphone, like Tempdrop, Ran's Night, iFever, and iSense (Figure 17).

Another innovative device to detect body temperature is the Smart Helmet, which is useful since it is safer than an infrared thermometer gun due to lower human interactions (Triaxtec, 2019). In this device, when the thermal camera detects the high temperature on the Smart Helmet, the position and

Figure 17: iFever (a), Tempdrop (b), iSense (c), Ran's Night (d), and smart thermometers.

the picture of the person's face are taken by an optical camera and transmitted to the determined mobile device with an alarm (Figure 18).

Moreover, Google Location History can be incorporated with the Smart Helmet to find the places attended by a suspected or infected person, and additionally can enhance further actions with more reliability by capturing the suspicious case sites (Calabrese et al., 2020).

Another example is Vuzix smart glasses (https://www.vuzix.com/) with the Onsight Cube thermal camera. These devices, produced by Vuxis, can monitor crowds to detect people who have high temperatures and send the information to the medical Center (Figure 19) (Mohammed et al., 2020).

Other studies have shown how, by using Unmanned Ariel Vehicles (UAVs) and in particular IoT-based drones, it is possible to speed up the process of finding people affected by CoVID-19 and monitor areas without risk of contamination (Chamola et al., 2020). There are various categories of the drone: Disinfectant Drone and Medical/Delivery Drone. An example is a drone shown in (Figure 20), designed to capture people's temperature in a crowd and be used in the early diagnosis phase.

Robots have also had a significant impact in this context, both for the diagnosis process by collecting swabs, and later to assist patients. An example of this device, the robot named Intelligent Care Robot (Figure 21) developed through a partnership between Vayyar Imaging and Meditemi companies. This robot allows detecting symptoms related to COVID-19 in 10 s using a quick scan without coming into contact with the patient.

Chamola et al. (2020), in association with the Cleveland Clinic, used physiological data, gathered via the wrist-mounted WHOOP Strap 3.0, from hundreds of WHOOP members who identified themselves as infected by COVID-19. The strap can notify the user of any issues that they might experience. This device also allows to remotely monitor the employees' health status and keep a record of any case of COVID-19

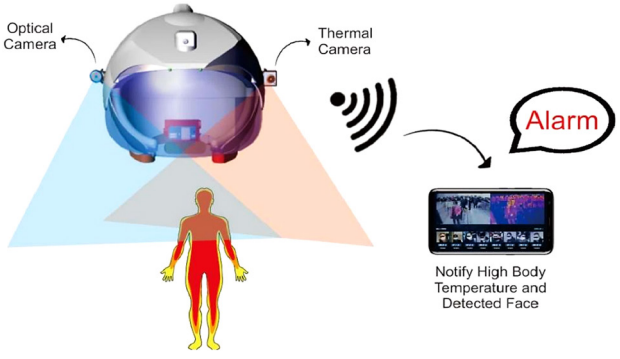

Figure 18: Smart Helmet captures temperature by the thermal optical camera (Triaxtec, 2019).

Figure 19: Smart glasses temperature capturing (Mohammed et al., 2020).

Figure 20: Thermal imaging drone (Hitconsultant, 2019).

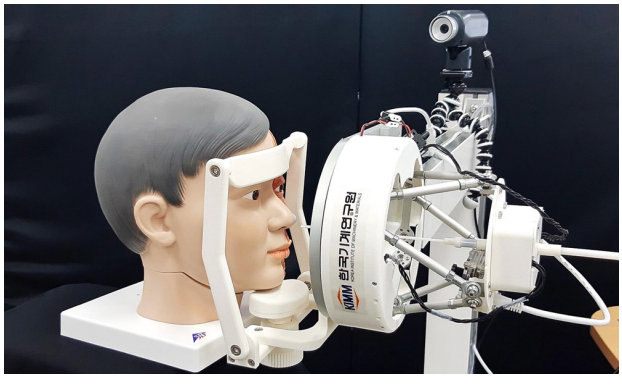

Figure 21: Autonomous swab test robots (South Korean Institute of Machinery and Material, 2019).

transmission amongst them. When this device is turned on, it scans for other wearable devices and records any close interactions with them. The device includes a passive GPS location-tracker and Bluetooth-based proximity sensors, ultra-wideband connectivity, built-in LTE (Long-Term Evolution), and a rechargeable battery. Since it is essential to control the disease spread, the wearer can update his health according to three different possibilities (certified healthy, symptomatic, or infected verified), recorded in a central database able to store information for up to 6 weeks. Rapid diagnosis of the COVID-19 can allow governments to take effective response measures to limit the virus spreading. The lack of testing kits in the world has made it hard for the authorities to carry out large-scale diagnostic testing. Therefore, to limit the exposure of frontline personnel to COVID-19 patients, many hospitals and airports have adopted the use of cameras with multi-sensory technology based on artificial intelligence (AI). These cameras allow authorities to observe crowds, identify people with high body temperatures, recognize their faces, and track their movements. For example, the Tampa General Hospital in Florida (USA) has installed a camera that uses AI technologies at its entrance to screen all patients entering the facility by performing a thermal scan of the face. The AI system uses ML of camera-detected results to classify whether or not an individual exhibits symptoms of COVID-19. In conclusion, voice detection is one of the easy technologies that can be employed to identify potential COVID-19 patients. During these difficult times, voice detection platforms can act as a screening measure to decide who needs to be tested.

Stojanović et al. (2020) presented a wearable system/device capable of tracking critical COVID-19 symptoms. It allows monitoring body temperature, heart rate, respiration rate, and other vital signs, which are essential to alert patients and remote medical staff about unusual symptoms correlated to COVID-19 or similar diseases. The simplest sensor consists of any mobile phone with a standard headset with a built-in microphone. It takes over breathing problems, respiration rate, and cough. It is attached to microphone/speakers input through the 3.5 mm jack. The built-in microphone records every audio signal on the mobile phone, then imported and processed with processing software, such as MATLAB, both in the time and frequency domain. It can detect the analyzed audio signal characteristics such as respiratory rate, rapid or shortened breathing, and cough. The user receives audio feedback via earphones, such as an audible alarm, when the respiratory rate is above or below the threshold, or some breathing problems such as rapid breathing or heavy cough, are present. The authors proposed another extended configuration, equipped with more sensors interfaced with a mobile app and managed by an Arduino board.

The temperature sensor (a PTC or NTC thermistor) is integrated into the earphone, whereas the heart rate sensor is in the form of Photoplethysmography (PPG) clips applied to the ear lobes. Respiratory rate and body temperature are measured by using the microphone and thermistor. The headset was then modified mounting the thermistor on the capsule's surface, and the second speaker was replaced with the PPG clip. Simple standard circuits amplify the signals based on operational amplifiers before they are acquired and processed by the Arduino. The significant part of the pre-processing (low and high pass filtering, envelope detection, signal smoothing, and threshold, etc.) is performed by amplifiers (Figure 22).

Filters are software implemented, in integer arithmetic, to be fast and with low memory usage. The locations of the heart rate and respiratory rate peaks are calculated from the spectrum obtained with the Fast Fourier Transform (FFT). Due to limited memory resources, FFT is implemented on the Arduino, with integer arithmetic. The microphone signal envelope detector is then implemented by the amplifiers, converting the audio signal into a low-frequency signal, reducing the sampling frequency to 25 Hz. The same sampling rate is used for processing the four signals. Figure 23 shows the Arduino interface based on signal acquisition filters.

Singh et al. (2020) developed an IoT-based wearable quarantine band (IoT-Q-Band) to detect absconding. Designing it, they kept in mind the cost, global supply chain disruption, and COVID-19 quarantine duration, according to the World Health Organization (WHO) recommendations. IoT-Q-Band is a low-cost solution that could benefit low-income regions to prevent the spread of COVID-19 (Figure 24).

This wearable prototype reports and tracks the absconding quarantine subjects in real-time through a mobile app. The wearable strap is worn by a quarantined subject on the hand, arm, or leg and connected through wireless to the mobile application via a Bluetooth link. After tampering with the band, the latter transmits the status (one byte of data) to the mobile application every 2 min. The subject will be registered in the IoT-Q-Band system by the relevant medical authority, responsible for the duration of the quarantine and other details. During the registration phase, the system stores the GPS coordinates of the position where the quarantine will be carried out. The mobile application provides the following visual

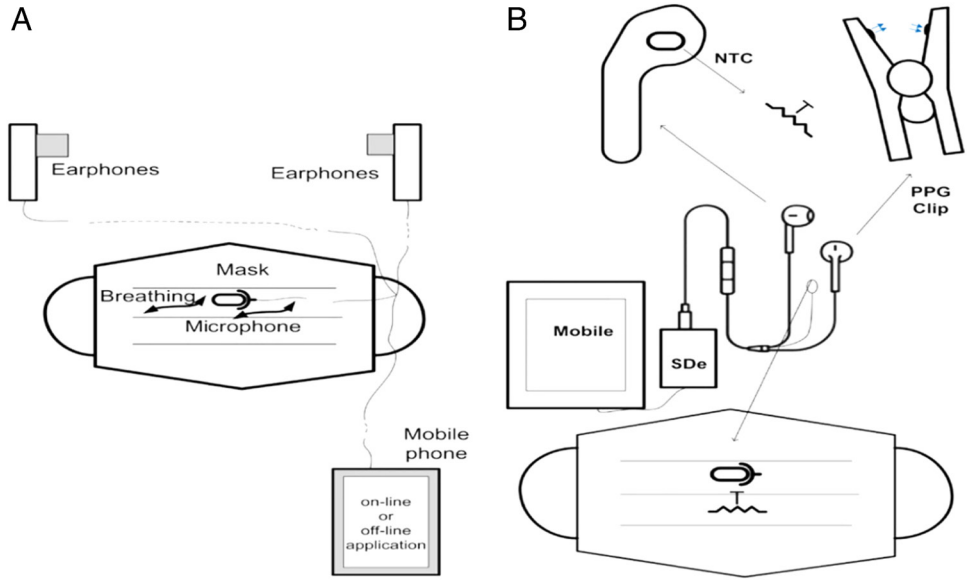

Figure 22: The configuration of the headset's microphone for the respiration rate and breathing detection, (a) configuration of the heart rate, temperature, and respiration rate detection using NTC thermistor, microphone, and PPG sensor, (b) (Stojanović et al., 2020).

feedback: (1) if the wearable strap is working or is tampered with, (2) if the subject is within 50 meters (geo-fencing) of the recorded quarantine location, and (3) the remaining time of quarantine. After the subject's registration, the mobile application pushes a Javascript Object Notation (JSON) packet to the cloud server containing information about the wearable band's state and GPS coordinates (Figure 25).

The IoT-Q-Band relies on the ESP32 chip sewn onto a 6 cm wide strip of fabric. It is covered so that the user is comfortable wearing it, and the tamper detection wire is soldered to a ground pin and sewn to the material. The other end of the tamper detection cable is plug-n-play and connects to a digital input/output (DIO) pin, programmed as an input (with the internal pull-up resistor enabled) (Figure 26).

The IoT-Q-Band is securely and comfortably attached to the wrist or legs with Velcro strips. IoT-Q-Band system has three visual indicators related to:

- The tampering of the IoT-Q-Band and the main indicator changes color from green to red;
- The drifting apart of the subject over 50 meters from the memorized quarantine position (during initial recording) and the central indicator changes color from green to red; and

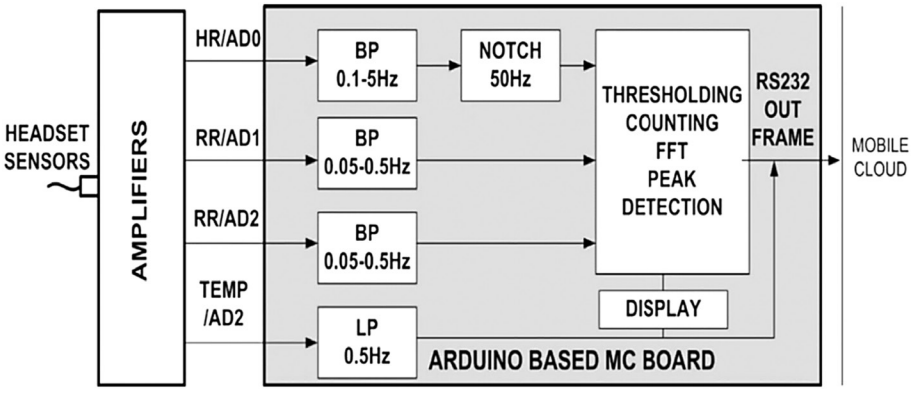

Figure 23: Block diagram of the Arduino based interface for processing vital signs (Stojanović et al., 2020).

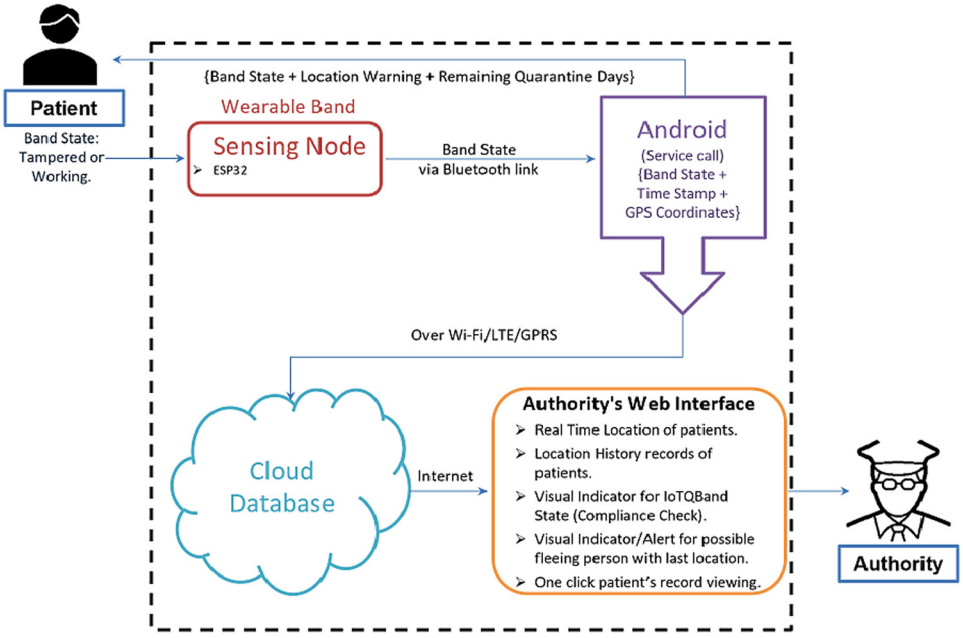

Figure 24: The system architecture of the IoT-Q-Band system (Singh et al., 2020).

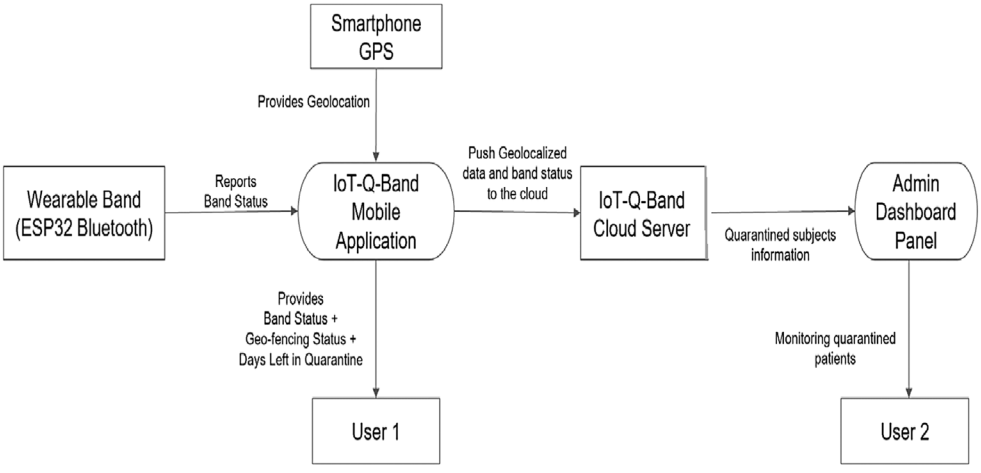

Figure 25: Data flow diagram of the IoT-Q-Band system (Singh et al., 2020).

- The patient data is not updated in the last 10 min (calculated based on the timestamp of the last received packet).

Finally, the authors discovered that while transmitting a byte of data, the current consumption stays at 100 mA for 8 s. In contrast, setting a detection period of 2 m, the IoT-Q-Band consumes 30 mA for 112 s and 100 mA for the next 8 s, and thus, the average current consumption by the band is just 34.66 mA. In addition, they found that the GPS location uncertainty reported through a smartphone generally depends on the surroundings or the measurement environment.

Han et al. (2019) proposed a new clustering model for medical applications (CMMA) to select the cluster head and provide energy-efficient communication in the telemedicine scenario. Specifically, the system

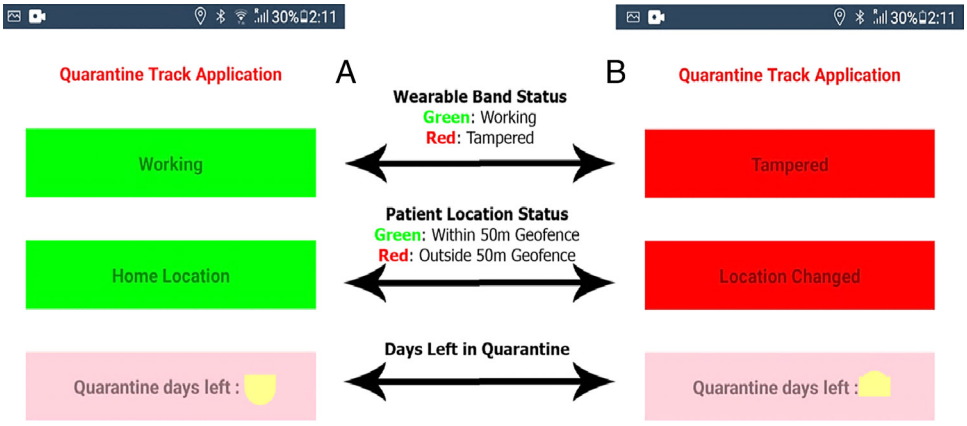

Figure 26: Mobile application screens of the IoT-Q-Band system showing the cases: (a) when the band is connected, and the subject is within 50 meters of registered quarantine Geo-location, and (b) when the wearable tampered, and the patient is outside the 50 meters of the registered quarantine Geo-location (Singh et al., 2020).

chooses the device with the higher remaining energy level and closer to the base station. The authors have demonstrated that the proposed CMMA presented better sustainability and energy-efficiency compared to other considered solutions (i.e. Low Energy Adaptive Clustering Hierarchy-LEACH, Particle Swarm Optimization-PSO, gravitational search algorithm-GSA). Furthermore, Fei et al. (2006) introduced a custom routing framework for collecting biophysical data from portable and wearable devices, allowing high-efficiency data queries. A crucial topic related to telemedicine IoT systems concerns information security, given the sensitivity of the data processed (Zhang et al., 2020). However, energy-efficient data encryption systems are needed since wearable, low-power, and battery-limited devices are typically involved in these applications (Pirbhulal et al., 2017). For instance, Pirbhulal et al. (2017) introduce an efficient and reliable IoT smart home automation system, supported by a WSN; the data encryption system employs a triangle-based security algorithm (TBSA) method to make efficient the key generation step. The developed proof-of-concept demonstrated that the proposed TBSA algorithm is more energy-efficient than other approaches. Similarly, Snader et al. (2016) created an energy-efficient, secure, and agnostic encryption protocol properly designed for IoT healthcare applications. The obtained results indicated excellent performances and reduced overhead, essential requirements for wearable or portable devices.

Currently, the WHO advises those in direct contact with coronavirus patients and with people who cough to wear a face mask. Stanford et al. (2019) described a self-cleaning filter composed of laser-induced graphene (LIG), which can capture bacteria and particulates, and a conductive graphene foam formed through the photothermal conversion of a polyimide film by a commercial CO2 laser cutter. This filter readily reaches a temperature greater than 300°C by a periodic Joule-heating mechanism. This mechanism can destroy bacteria and molecules that cause adverse biological reactions and diseases (pyrogens, allergens, exotoxins, endotoxins, mycotoxins, nucleic acids, and prions). Using thermal stability and the high surface area of LIG, the utility of graphene for reducing infection in hospital settings is suggested. This filter shows a modest electrical conductivity that enables the filter to be Joule-heated by electrical power dissipation. Figure 27 shows the filter testing setup and the working principle for self-sterilization of the filter.

The authors demonstrated that LIG can capture bacteria and prevents proliferation, even when submerged in a culture medium. The filter overcomes the traditional filters and disinfection methods, as the self-sterilization by Joule-heating can avoid the accumulation of microorganisms on the filter and subsequent downstream contamination.

A new graphene-based mask named Guardian G-Volt, produced by LIGC Applications, is based on the same principle above described (Figure 28) (Dezeen, 2019). LIGC Applications claims that the adopted graphene-based filtration system is 99% effective against particles over 0.3 µm and 80% against anything smaller. Compared to an N95 breathing mask, it blocks 95% of particles over 0.3 µm. A low-level current will pass through the Guardian G-Volt when connected to a portable

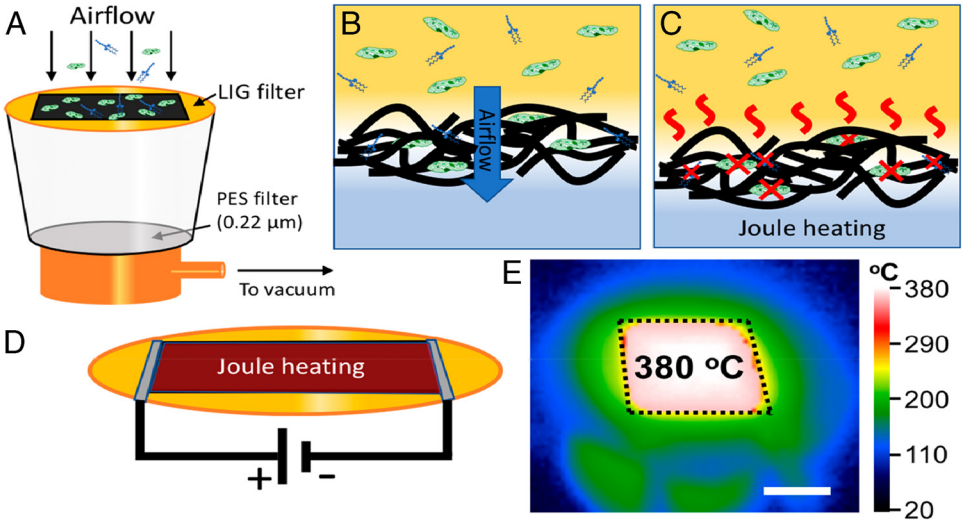

Figure 27: Representation of filter testing setup and the working principle for self-sterilization of the filter (Stanford et al., 2019).

Figure 28: Example of the Guardian G-Volt mask application (Dezeen, 2019).

battery pack via a USB port. This charge would repel the particles trapped in the graphene mask. At home, a docking system allows the mask to be sterilized, to be worn again. Graphene, a material with impressive characteristics, is naturally antibacterial, so Guardian G-Volt can also protect the wearer from bacteria. The graphene in the mask is a type called LIG. This microporous conductive foam can trap bacteria and conduct the electricity needed to sterilize the mask's surface.

Another significant step beyond has been done by Philips, which developed a next-generation wearable biosensor to detect patient deterioration, including clinical surveillance for COVID-19 (Philips, 2019). The Philips Biosensor BX100 (Figure 29a) enhances clinical supervision of patient deterioration, reducing the risk to intervene earlier and improving care for patients in low acuity care areas. The solution received a CE mark and is currently in use at the *Onze Lieve Vrouwe Gasthuis* (OLVG) hospital in the Netherlands to monitor COVID-19 patients.

The Philips Biosensor BX100 is designed to address a new approach to vital signs measurements. It is a single-use wearable patch with 5-day autonomy, combined with a scalable hub to monitor several patients across multiple rooms. The scheme related to the monitoring system's operation is reported in Figure 29c.

The Philips Biosensor BX100 device does not require cleaning or charging and can be included in existing clinical workflows for surveillance and notifications tasks. The wireless wearable biosensor is applied to the chest (Figure 29b). Every minute, it enables to collect, measure, store, and send respiratory rate, heart rate, and contextual parameters (i.e., posture and activity level).

Performance and comparative analysis of discussed systems, sensors, and technologies

This section provides a comparative analysis of the sensing solutions and technologies described in the second section, for detecting patients affected by the COVID-19 virus, pointing out the performance

Figure 29: BX100 Philips Biosensor (Philips, 2019): front view of the device (a), and its application on a patient (b), the graphical scheme of the health monitoring system (c).

evaluation mechanisms, application scenarios, target species, advantages, and limitations, to determine the most promising tools to face future pandemics.

In the second section, we have extensively analyzed the different magnetic biosensor technologies, which shows, also at low analyte's concentration, higher sensitivity than other detection methods, such as the standard fluorescent system (Schotter et al., 2004). Furthermore, the magnetic biosensors present a lower background noise compared to other sensor technologies, such as the optical-based ones (Srinivasan et al., 2009), and intrinsic compatibility with the micro and nanofabrication technologies, making them suitable for the realization of sensor arrays on a single chip enabling parallel detection. The MR biosensors, including GMR and NMR, are typically featured by moderate MR ratio and good linearity, but suffer from intrinsic fragility and reduced MR ratio at high temperature. The electrochemical biosensors are featured by high sensitivity, fast response time, good selectivity, and simple miniaturization (Menon et al., 2020). However, this biosensors typology shows a limited shelf life, and a sensitivity affected by sample matrix and temperature, inducing the antibodies deterioration, thus corrupting the sensor operation. The plasmonic biosensors are very sensitive to small sample changes and repeatable, as well as do not require a calibration model given to the conventional electrical model (Villena Gonzales et al., 2019). However, they are susceptible to motion, temperature, and sweat, and need a long calibration process.

Given the advantages and disadvantages of the analyzed technologies, the next step is to compare the scientific works discussed in the second section to bring out differences and potentialities for defining the future generation of rapid virus' assay methods. Table 3 shows a comparison between different biosensors and bio-detectors in terms of the detection technology, target species, LOD, application scenario, and scalability, intended as the ability of the detection system to be applied to a broad audience of users.

Specifically, despite their high sensitivity, the GMR and NMR detection methods are time-consuming, require multiple washing steps during the detection process, hence the use of specialized staff, and involve a high cost for every test, taking into account the bio-detector cost, thus reducing the technology scalability. The NMR detection method is typically featured by a sensitivity lower than both GMR and MPS techniques, entailing the same practical issues related to the washing steps, that reduce the system sensitivity.

Table 3. Comparison between the scientific works reported in the second section, in terms of the detection technology, target species, LOD, detection time, application scenario and scalability.

Scientific work	Detection mechanism	Target species	LOD	Detection time	Application scenario	Scalability
Wu et al. (2020)	GMR	H1N1 virus H3N2 virus	15 ng/mL 125 TCID50/ml	10 min	Virus screening	Low
Orlov et al. (2016)	MPS	BoNT A, B and E	0.22, 0.11, 0.32 ng/mL	25 min	Food quality	Medium
Zhang et al. (2013)	MPS	ssDNA	400 pM	10 sec	DNA analysis	Medium
Lei et al. (2015)	NMR	$CuSO_4$	0.2 µM	1 min	cell isolation, cell culture, DNA amplification	Medium
Zhao et al. (2021)	electrochemical	SARS-CoV-2 virus	200 copies/mL	10 sec	Virus screening	High
Vadlamani et al. (2020)	electrochemical	SARS-CoV-2 virus	14 nM	30 sec	Virus screening	High
Chin et al. (2017)	electrochemical	JEV virus	5–20 ng/mL	20 min	Virus screening	High
Seo et al. (2020)	FET-based	SARS-CoV-2 virus	1.7 fM	20 sec	Virus screening	High
Moitra et al. (2020)	LSPR	SARS-CoV-2	0.18 ng/µL	10 min	Virus screening	Low

The electrochemical biosensors are considered one of the most promising clinical diagnosis and point-of-care detection technologies, essential for applications such as rapid drug tests, food monitoring, glucose detection, etc. (Menon et al., 2020). Their compatibility with fabrication techniques, like screen printing based on carbon nanoparticles, opens a new frontier toward developing low-cost, reliable, rapid, and disposable clinical tests that offer results similar to the standard approaches (Chin et al., 2017). The FET-based biosensors provide numerous benefits, like high sensitivity and the capability to carry out real-time measurements with a reduced amount of analytes. Besides, the graphene-based FET biosensors represent a promising solution for realizing biological assays for clinical diagnosis of diseases, such as cardiac diseases, kidney injury, diabetes, cancers, inflammatory, and infectious diseases, exploiting the conductivity and large area featuring the graphene. These devices show optimum sensitivity, real-time detection, and low production costs, allowing the realization of disposable biological assays for mass screening in pandemics or other diseases. In the last years, several efforts have been made for overcoming some issues affecting the FET-based biosensors related to sensitivity and response time due to the minimum obtainable subthreshold swing (Sarkar and Banerjee 2012). The SPR and LSPR biosensors are characterized by very high sensitivity, accuracy, and real-time detection of unknown analytes (Esfahani Monfared, 2020). Nevertheless, the plasmonic biosensors usually employ an optical substrate in the form of a glass/polymer prism to couple the light emitted by a laser source with the surface oscillations, an arrangement known as the Kretschmann configuration. This configuration is bulky and difficult to integrate into a compact setup, reducing the applicability of plasmonic biosensors for POC testing.

Conclusions

The manuscript aims to explore the technologies and systems employed to fight against COVID-19 diffusion. At first, we investigated the methodologies

and the related instrumentations to carry out rapid and reliable assays to identify the infected subject, thus breaking the contagion chain. Specifically, we focused on the magnetic biosensors technologies, including MR sensors, MPS, and NMR platforms, offering several advantages compared to plasmonic, electrochemical, and optical sensors, such as lower background noise and influence of sample matrix typology. Furthermore, magnetic-based detection sensors can be easily combined with compact and portable readers, thanks to the availability of a low-cost and high-performance processing platform, allowing the rapid testing of large numbers of people. Besides, we have analyzed novel solutions of electrochemical and plasmonic biosensors for detecting the SARS-CoV-2 virus, featured by high reliability and low-cost. To become competitive with other analysis techniques (e.g., fluorescent spectroscopy), it is needed to investigate functionalized magnetic nanomaterials to carry out a multi-analyte detection strategy. Besides, in the next future, we forecast the development of fully integrated, disposable, and label-free magnetic sensors without the need for an MNP detector; these biosensors require the implementation of novel and low-cost microfluidic structures and a suitable integration of the electronic sections. Thanks to their potentialities, the electrochemical biosensors represent the most promising solution for point-of-care and rapid diagnosis of infectious diseases to contain future pandemics. However, the development of new engineered nanomaterials for signal amplification constitutes a powerful solution for improving device performances (Kumar et al., 2019). The SPR instrumentations are still relatively cumbersome and expensive, making them not adequate for a portable diagnosis system. Therefore, several studies must be addressed to integrate alternative light sources (e.g., LEDs) and detectors (e.g., CMOS sensors) to reduce the size and cost of the SPR detector (Liu et al., 2015). A further challenge to be faced concerns the limited multiplexing capability of SPR devices, which requires multi-sensor chips and multiple microfluidic sensing channels (Li et al., 2020; Taylor et al., 2006).

Also, the latest devices and IoT architectures for containing the COVID-19 spreading have been investigated. In particular, we analyzed the solutions for limiting the contagion, and those to rapidly screen a large number of people for detecting the suspected people based on the symptoms featuring the COVID-19 infection, such the fever and breathing problems. Furthermore, we explored innovative IoT frameworks for remotely detecting and monitoring the user's vital signs to prevent and eradicate the COVID-19 virus or similar disease.

Literature Cited

Afzal, A. 2020. Molecular diagnostic technologies for COVID-19: limitations and challenges. *Journal of Advanced Research* 26: 149–159.

Baselt, D. R., Lee, G. U., Natesan, M. S., Metzger, W., Sheehan, P. E. and Colton, R. J. 1998. A biosensor based on magnetoresistance technology. *Biosensors and Bioelectronics* 13(7): 731–739.

Blümich, B. 2016. Introduction to compact NMR: a review of methods. *TrAC Trends in Analytical Chemistry* 83: 2–11, available at: https://doi.org/10.1016/j.trac.2015.12.012.

Calabrese, B., Velázquez, R., Del-Valle-Soto, C., de Fazio, R., Giannoccaro, N. I. and Visconti, P. 2020. Solar-powered deep learning-based recognition system of daily used objects and human faces for assistance of the visually impaired. *Energies* 13(22): 1–30, available at: https://doi.org/10.3390/en13226104.

Chamola, V., Hassija, V., Gupta, V. and Guizani, M. 2020. A comprehensive review of the covid-19 pandemic and the role of IoT, drones, AI, blockchain, and 5G in managing its impact. *IEEE Access* 8: 90225–90265, available at: https://doi.org/10.1109/ACCESS.2020.2992341.

Charibaldi, N., Harjoko, A., Azhari, A. and Hisyam, B. 2018. A new HGA-FLVQ model for Mycobacterium tuberculosis detection. *International Journal on Smart Sensing and Intelligent Systems* 11(1): 1–13, available at: https://doi.org/10.21307/ijssis-2018-028.

Chin, S. F., Lim, L. S., Pang, S. C., Sum, M. S. H. and Perera, D. 2017. Carbon nanoparticle modified screen printed carbon electrode as a disposable electrochemical immunosensor strip for the detection of Japanese encephalitis virus. *Microchimica Acta* 184: 491–497, available at: https://doi.org/10.1007/s00604-016-2029-7.

Choi, J., Gani, A. W., Bechstein, D. J. B., Lee, , J., Utz, P. J. and Wang, S. X. 2016. Portable, one-step, and rapid GMR biosensor platform with smartphone interface. *Biosensors and Bioelectronics* 85: 1–7, available at: https://doi.org/10.1016/j.bios.2016.04.046.

de Fazio, R., Cafagna, D., Marcuccio, G., Minerba, A. and Visconti, P. 2020. A multi-source harvesting system applied to sensor-based smart garments for monitoring workers' bio-physical parameters in harsh environments. *Energies* 13: 1–33, available at: https://doi.org/10.3390/en13092161.

Dezeen. 2019. "Guardian G-Volt masks use graphene and electrical charge to repel viruses", [Online] available at: https://www.dezeen.com/2020/03/06/guardian-g-volt-face-mask-graphene-coronavirus-bacteria/ (Accessed December 21, 2020).

Esfahani Monfared, Y. 2020. Overview of recent advances in the design of plasmonic fiber-optic biosensors. *Biosensors* 10: 77, available at: https://doi.org/10.3390/bios10070077.

Fei, H., Yu, W. and Hongyi, W. 2006. Mobile telemedicine sensor networks with low-energy data

query and network lifetime considerations. *IEEE Transactions on Mobile Computing* 5: 404–417, available at: https://doi.org/10.1109/TMC.2006.1599408.

Gaetani, F., de Fazio, R., Zappatore, G. A. and Visconti, P. 2020. A prosthetic limb managed by sensors-based electronic system: experimental results on amputees. *Bulletin of Electrical Engineering and Informatics* 9(2): 514–524, available at: https://doi.org/10.11591/eei.v9i2.2101.

Gaetani, F., Primiceri, P., Zappatore, G. A. and Visconti, P. 2019. Hardware design and software development of a motion control and driving system for transradial prosthesis based on a wireless myoelectric armband. *IET Science, Measurement Technology* 13(3): 354–362, available at: https://doi.org/10.1049/iet-smt.2018.5108.

Grancharov, S. G., Zeng, H., Sun, S., Wang, S. X., O'Brien, S., Murray, C., Kirtley, J. and Held, G. 2005. Bio-functionalization of monodisperse magnetic nanoparticles and their use as biomolecular labels in a magnetic tunnel junction based sensor. *Journal of Physical Chemistry B* 109(26): 13030–13035, available at: https://doi: 10.1021/jp051098c.

Hajian, R., Balderstone, S., Tran, T., deBoer, T., Etienne, J., Sandhu, M., Wauford, N. A., Chung, J., Nokes, J., Athaiya, M., Paredes, J., Peytavi, R., Goldmsmith, B., Murthy, N., Conboy, I. M. and Aran, K. 2019. Detection of unamplified target genes via CRISPR–Cas9 immobilized on a graphene field-effect transistor. *Nature Biomedical Engineering* 3: 427–437, available at: https://doi:10.1038/s41551-019-0371-x.

Hale, W., Rossetto, G., Greenhalgh, R., Finch, G. and Utz, M. 2018. High-resolution nuclear magnetic resonance spectroscopy in microfluidic droplets. *Lab on a Chip* 18(19): 3018–3024, available at: https://doi.org/10.1039/C8LC00712H.

Han, T., Zhang, L., Pirbhulal, S., Wu, W. and Albuquerque, V. 2019. A novel cluster head selection technique for edge-computing based IoMT systems. *Computer Networks* 158: 114–122, available at: https://doi.org/10.1016/j.comnet.2019.04.021.

Hernández, S. and Sallis, P. 2020. Robust single target tracking using determinantal point process observations. *International Journal on Smart Sensing and Intelligent Systems* 13(1), available at: https://doi.org/10.21307/ijssis-2020-001.

Hitconsultant. 2019. "Draganfly Inc. Products-Smart Pandemic Drone", [Online], available at: https://hitconsultant.net/2020/03/27/pandemic-drone-could-detect-virus-symptoms-like-covid-19-in-crowds/#.X9cyIVVKjIX (Accessed February 21, 2019).

Jatmiko, W., Anwar Ma'sum, M., Arief Wisesa, H. and Rolis Sanabila, H. 2019. Developing smart Tele-ECG system for early detection and monitoring heart diseases based on ECG signal: progress and challenges. *International Journal on Smart Sensing and Intelligent Systems* 12(1): 1–12, available at: https://doi.org/10.21307/ijssis-2019-009.

Jeyaprakash, T. and Mukesh, R. 2015. An optimized node selection routing protocol for vehicular ad-hoc networks – a hybrid model. *Journal of Communications Software and Systems* 11(2): 80–85, available at: https://doi.org/10.24138/jcomss.v11i2.106.

Jung, I. Y., You, J. B., Choi, B. R., Kim, J. S., Lee, H. K., Jang, B., Jeong, S. H., Lee, K., Im, S. G. and Lee, H. 2016. A highly sensitive molecular detection platform for robust and facile diagnosis of Middle East Respiratory Syndrome (MERS) corona virus. *Advanced Healthcare Materials* 5(17): 2168–2173, available at: https://doi.org/10.1002/adhm.201600334.

Jung, Y. 2020. A review of privacy-preserving human and human activity recognition. *International Journal on Smart Sensing and Intelligent Systems* 13(1): 1–13, available at: https://doi.org/10.21307/ijssis-2020-008.

Kumar, A., Purohit, B., Maurya, P. K., Pandey, L. M. and Chandra, P. 2019. Engineered nanomaterial assisted signal-amplification strategies for enhancing analytical performance of electrochemical biosensors. *Electroanalysis* 31: 1615–1629, available at: https://doi.org/10.1002/elan.201900216.

Lassoued, H., Ketata, R. and Yacoub, S. 2018. ECG decision support system based on feedforward neural networks. *International Journal on Smart Sensing and Intelligent Systems* 11(1): 1–13, available at: https://doi.org/10.21307/ijssis-2018-029.

Lay-Ekuakille, A., Visconti, P., de Fazio, R. and Veneziano, D. 2019. Quasi-real time acquisition and processing for biomedical IR and conventional imaging in surgery applications. *Journal of Instrumentation* 14(P03011): 1–8, available at: https://doi.org/10.1088/1748-0221/14/03/P03011.

Lei, K. M., Mak, P. I., Law, M. K. and Martins, R. P. 2015. A palm-size μNMR relaxometer using a digital microfluidic device and a semiconductor transceiver for chemical/biological diagnosis. *Analyst* 140: 5129–5137, available at: https://doi.org/10.1039/C5AN00500K.

Li, J., Han, D., Zeng, J., et al. 2020. Multi-channel surface plasmon resonance biosensor using prism-based wavelength interrogation. *Optics Express* 28: 14007–14017, available at: https://doi.org/10.1364/OE.389226.

Li, M., Cushing, S. K. and Wu, N. 2015. Plasmon-enhanced optical sensors: a review. *Analyst* 140: 386–406, available at: https://doi.org/10.1039/c4an01079e.

Liu, Y., Liu, Q., Chen, S., Cheng, F., Wang, H. and Peng, W. 2015. Surface plasmon resonance biosensor based on smart phone platforms. *Scientific Reports* 5: 12864, available at: https://doi.org/10.1038/srep12864.

Maghded, H., Ghafoor, K., Sadiq, A. S., Curran, K., Rawat, D. B. and Rabie, K. 2020. *A Novel AI-enabled Framework to Diagnose Coronavirus COVID 19 using Smartphone Embedded Sensors: Design Study* 2020 IEEE International Conference on Information Reuse and Integration for Data Science (IRI), Las Vegas, NV, August, pp. 180–187, available at: https://doi.org/10.1109/IRI49571.2020.00033.

Mahari, S., Roberts, A., Shahdeo, D. and Gandhi, S. 2020. eCovSens-Ultrasensitive Novel In-house built printed circuit board based electrochemical device for rapid detection of nCovid-19 antigen, a spike protein domain 1 of SARS-CoV-2. *BioRxiv* 1(1): 1–20, available at: https://doi.org/10.1101/2020.04.24.059204.

Mauriz, E. 2020. Recent progress in plasmonic biosensing schemes for virus detection. *Sensors* 20(17): 1–27, available at: https://doi.org/10.3390/s20174745.

Mbuthia, K., Dai, J., Zavrakas, S. and Yan, J. 2018. Patient-centric healthcare data processing using streams and asynchronous technology. *International Journal on Smart Sensing and Intelligent Systems* 11(1): 1–18, available at: https://doi.org/10.21307/ijssis-2018-003.

Menon, S., Mathew, M. R., Sam, S., Keerthi, K. and Girish Kumar, K. 2020. Recent advances and challenges in electrochemical biosensors for emerging and re-emerging infectious diseases. *Journal of Electroanalytical Chemistry* 878: 1–14, available at: https://doi.org/10.1016/j.jelechem.2020.114596.

Mohammed, M. N., Hazairin, N. A., Syamsudin, H. and Al-Zubaidi, S. 2020. 2019 Novel Coronavirus Disease (Covid-19): detection and diagnosis system using IoT based smart glasses. *International Journal of Advanced Science and Technology* 29(7): 954–960.

Moitra, P., Alafeef, M., Dighe, K., Frieman, M. B. and Pan, D. 2020. Selective naked-eye detection of SARS-CoV-2 mediated by N gene targeted antisense oligonucleotide capped plasmonic nanoparticles. *ACS Nano* 14(6): 7617–7627, available at: https://doi.org/10.1021/acsnano.0c03822.

Nasajpour, M., Pouriyeh, M., Parizi, S., Dorodchi, R. M., M., Valero, M. and Arabnia, H. R. 2020. Internet of things for current COVID-19 and future pandemics: an exploratory study. *Journal of Healthcare Informatics Research* 4: 325–364, available at: https://doi.org/10.1007/s41666-020-00080-6.

Orlov, A. V., Znoyko, S. L., Cherkasov, V. R., Nikitin, M. P. and Nikitin, P. I. 2016. Multiplex biosensing based on highly sensitive magnetic nanolabel quantification: rapid detection of botulinum neurotoxins A, B, and E in liquids. *Analytical Chemistry* 88(21): 10419–10426, available at: https://doi.org/10.1021/acs.analchem.6b02066.

Otoom, M., Otoum, N., Alzubaidi, M. A., Etoom, Y. and Banihani, R. 2020. An IoT-based framework for early identification and monitoring of COVID-19 cases. *Biomedical Signal Processing and Control* 62: 1–9, available at: https://doi.org/10.1016/j.bspc.2020.102149.

Park, G. S., Ku, K., Baek, S. H., Kim, S. -J., Kim, S. I., Kim, B. -T. and Maeng, J. -S. 2020. Development of reverse transcription loop-mediated isothermal amplification assays targeting severe acute respiratory syndrome coronavirus 2 (SARS-CoV-2). *The Journal of Molecular Diagnostics* 22(6): 729–735, available at: https://doi.org/10.1016/j.jmoldx.2020.03.006.

Philips. 2019. "Biosensor BX100", [Online], available at: https://www.philips.it/healthcare/product/HC989803203011/dispositivo-di-misurazione-in-remoto-indossabile-biosensor-bx100 (Accessed February 21, 2019).

Pietschmann, J., Vöpel, N., Spiegel, H., Krause, H. -J. and Schröper, F. 2020. Brief communication: magnetic immuno-detection of SARS-CoV-2 specific antibodies. *BioRxiv* 1: 1–16, available at: https://doi.org/10.1101/2020.06.02.131102.

Pirbhulal, S., Zhang, H. E., Alahi, M. E., Ghayvat, H., Mukhopadhyay, S., Zhang, Y. -T. and Wu, W. 2017. A novel secure IoT-based smart home automation system using a wireless sensor network. *Sensors* 17: 1–19, available at: https://doi.org/10.3390/s17010069.

Samson, R., Navale, G.R. and Dharne, M. S. 2020. Biosensors: frontiers in rapid detection of COVID-19. *3 Biotech* 10(9): 1–9, available at: https://doi.org/10.1007/s13205-020-02369-0.

Sarkar, D. and Banerjee, K. 2012. "Fundamental limitations of conventional-FET biosensors: Quantum-mechanical-tunneling to the rescue", *70th Device Research Conference* IEEE, University Park, PA, pp. 83–84.

Schotter, J., Kamp, P. B., Becker, A., Pühler, A., Reiss, G. and Brückl, H. 2004. Comparison of a prototype magnetoresistive biosensor to standard fluorescent DNA detection. *Biosensors and Bioelectronics* 19: 1149–1156, available at: https://doi.org/10.1016/j.bios.2003.11.007.

Seo, G., Lee, G., Kim, M. J., Baek, S. -H., Choi, M., Ku, K. B., Lee, C. -S., Parl, J. D., Kim, H. G., Kim, S. -J., Lee, J. -O., Kim, B. T., Parl, E. C. and Kim, S. I. 2020. Rapid detection of COVID-19 causative virus (SARS-CoV-2) in human nasopharyngeal swab specimens using field-effect transistor-based biosensor. *ACS Nano* 14: 5135–5142, available at: https://doi.org/10.1021/acsnano.0c02823.

Singh, V., Chandna, H., Kumar, A., Kumar, S., Upadhyay, N. and Utkarsh, K. 2020. IoT-Q-Band: A low cost internet of things based wearable band to detect and track absconding COVID-19 quarantine subjects. *EAI Endorsed Transactions on Internet of Things* 6(21): 1–9, available at: https://doi.org/10.4108/eai.13-7-2018.163997.

Smits, J., Damrom, J. T., Kehayias, P., McDowell, A. F., Mosavian, N., Descenko, I., Ristoff, N., Laraoui, A., Jarmola, A. and Acosta, V. 2019. Two-dimensional nuclear magnetic resonance spectroscopy with a microfluidic diamond quantum sensor. *Science Advances* 5(7): 1–7, available at: https://doi.org/10.1126/sciadv.aaw7895.

Snader, R., Kravets, R. and Harris, A. F. 2016. CryptoCoP: Lightweight, Energy-efficient Encryption and Privacy for Wearable Devices. In: Proceedings of the 2016 Workshop on Wearable Systems and Applications Association for Computing Machinery, New York, NY, pp. 7–12.

South Korean Institute of Machinery and Material 2019. "Robots offer a contact-free way of getting swabbed for coronavirus" [Online], available at: https://www.standard.co.uk/tech/robots-offer-new-coronavirus-swab-technique-a4477396.html (Accessed February 21, 2019).

Srinivasan, B., Li, Y., Jing, Y., Xu, Y., Yao, X., Xing, C. and Wang, J. -P. 2009. A detection system based on giant magnetoresistive sensors and high-moment magnetic nanoparticles demonstrates zeptomole sensitivity: potential for personalized medicine. *Angewandte Chemie International Edition* 48: 2764–2767, available at: https://doi.org/10.1002/anie.200806266.

Stanford, M. G., Li, J. T., Chen, Y., McHugh, E. A., Liopo, A., Xiao, H. and Tour, J. M. 2019. "Self-sterilizing laser-induced graphene bacterial air filter", *ACS Nano* 13(10): 11912–11920, available at: https://doi.org/10.1021/acsnano.9b05983.

Stojanović, R., Škraba, A. and Lutovac, B. 2020. *A Headset Like Wearable Device to Track COVID-19 Symptoms* 2020 IEEE Mediterranean Conference on Embedded Computing (MECO), Budva, Montenegro, 1–4, doi: 10.1109/MECO49872.2020.9134211.

Sun, S., Folarin, A., Ranjan, Y., Rashid, Z., Conde, P., Stewart, C., Matcham, N., Dalla Costa, G., Simblett, S., Leocani, L., Lamers, F., Sorensen, P. S., Buron, M., Zabalta, A., Myin-Germeys, I., Rintala, A., Wykes, T., Narayan, V. A., Comi, G., Hotopf, M. and Dobson, R. J. 2020. Using smartphones and wearable devices to monitor behavioural changes during COVID-19. *Journal Med Internet Res* 22(9): 1–11, available at: https://doi.org/10.2196/19992.

Taylor, A. D., Ladd, J., Yu, Q., Shengfu, C., Jiří, H. and Shaoyi, J. 2006. Quantitative and simultaneous detection of four foodborne bacterial pathogens with a multi-channel SPR sensor. *Biosensors and Bioelectronics* 22: 752–758, available at: https://doi.org/10.1016/j.bios.2006.03.012.

Triaxtec. 2019. "Proximity Trace TM: brochure" [Online], available at: https://www.triaxtec.com/social-distancing-contact-tracing/ (Accessed February 21, 2019).

Vadlamani, B. S., Uppal, T., Verma, S. C. and Misra, M. 2020. Functionalized TiO2 nanotube-based electrochemical biosensor for rapid detection of SARS-CoV-2. *Sensors* 20(20): 1–10, available at: https://doi.org/10.3390/s20205871.

Villena Gonzales, W., Mobashsher, A. T. and Abbosh, A. 2019. The progress of glucose monitoring–a review of invasive to minimally and non-invasive techniques, devices and sensors. *Sensors* 19: 1–45, available at: https://doi.org/10.3390/s19040800.

Visconti, P., de Fazio, R., Costantini, P., Miccoli, S. and Cafagna, D. 2019. Arduino-based solution for in-car-abandoned infants' controlling remotely managed by smartphone application. *Journal of Communications Software and Systems* 15(2): 89–100, available at: https://doi.org/10.24138/jcomss.v15i2.691.

Visconti, P., de Fazio, R., Costantini, P., Miccoli, S. and Cafagna, D. 2020. Innovative complete solution for health safety of children unintentionally forgotten in a car: a smart Arduino-based system with user app for remote control. *IET Science, Measurement Technology* 14(6): 665–675, available at: https://doi.org/10.1049/iet-smt.2018.5664.

Visconti, P., Gaetani, F., Zappatore, G. A. and Primiceri, P. 2018. Technical features and functionalities of Myo Armband: an overview on related literature and advanced applications of myoelectric armbands mainly focused on arm prostheses. *International Journal on Smart Sensing and Intelligent Systems* 11: 1–25, available at: https://doi.org/10.21307/ijssis-2018-005.

Wu, K., Klein, T., Krishna, V. D., et al. 2017. Portable GMR handheld platform for the detection of Influenza A Virus. *ACS Sensors* 2: 1594–1601, available at: https://doi.org/10.1021/acssensors.7b00432.

Wu, K., Saha, R., Su, D., Krishna, V. D., Liu, J., Cheeran, J. and Wang, J. 2020. Magnetic-nanosensor-based virus and pathogen detection strategies before and during COVID-19. *ACS Applied Nano Materials* 3(10): 9560–9580.

Yu, L., Wu, S., Hao, X., Dong, X., Mao, L., Pelechano, V., Chen, W. -H. and Yin, X. 2020. Rapid detection of COVID-19 coronavirus using a reverse transcriptional loop-mediated isothermal amplification (RT-LAMP) diagnostic platform. *Clinical Chemestry* 66(7): 975–977, available at: https://doi.org/10.1093/clinchem/hvaa102.

Zhang, J., Liu, H. and Ni, L. 2020. A Secure energy-saving communication and encrypted storage model based on RC4 for EHR. *IEEE Access* 8: 38995–39012, available at: https://doi.org/10.1109/ACCESS.2020.2975208.

Zhang, X., Reeves, D. B., Perreard, I. M., Kett, W., Grisworld, K. E., Gimi, B. and Weaver, J. B. 2013. Molecular sensing with magnetic nanoparticles using magnetic spectroscopy of nanoparticle Brownian motion. *Biosensors and Bioelectronics* 50: 441–446, available at: https://doi.org/10.1016/j.bios.2013.06.049.

Zhao, H., Liu, F., Xie, W., Zhou, T. -C., Yang, J. O., Li, H., Zhao, C. -Y., Zhang, L., Wei, J., Zhang, Y. -P. and Li, C. -P. 2021. Ultrasensitive supersandwich-type electrochemical sensor for SARS-CoV-2 from the infected COVID-19 patients using a smartphone. *Sensors and Actuators B: Chemical* 327: 1–9, available at: https://doi.org/10.1016/j.snb.2020.128899.

Zhou, P., Yang, X. L., Wang, X. G., Hu, B., Zhang, L., Zhang, W., Si, H. -R., Zhu, Y., Bei, L., Huang, C. -L., Chen, H. -L., Chen, H. -D., Chen, J., Luo, Y., Guo, H., Jiang, R., Liu, M. -Q., Shen, X., Wang, X., Zheng, X. -S., Zhao, K., Chen, Q. -J., Deng, F., Liu, L. -L., Yan, B., Zhan, F. X., Wang, Y. -Y., Xiao, G. -F. and Shi, Z. -L. 2020. A pneumonia outbreak associated with a new coronavirus of probable bat origin. *Nature* 579: 270–273, available at: https://doi.org/10.1038/s41586-020-2012-7.

Zuo, X., Fan, C. and Chen, H. -Y. 2017. Biosensing: CRISPR-powered diagnostics. *Nature Biomedical Engineering* 1: 91, available at: https://doi.org/10.1038/s41551-017-0091.